

Final Report
NO1-DC-6-2111
**The Neurophysiological Effects of
Simulated Auditory Prosthesis
Stimulation**

P.J. Abbas, J.T. Rubinstein, C.A. Miller, A.J. Matsuoka, B.K. Robinson

Department of Otolaryngology - Head and Neck Surgery
Department of Speech Pathology and Audiology
Department of Physiology and Biophysics
University of Iowa
Iowa City, IA 52242

November 1, 1999

Contents

1	Introduction	1
2	Characteristics of the EAP	1
2.1	Morphology and growth	1
2.2	Strength-duration function	4
2.3	Response to pseudomonophasic pulses	5
2.4	Recovery of the EAP from forward masking	5
2.5	Channel interaction	6
2.6	EAP responses to pulse-trains	9
2.7	Conduction velocity estimate	12
2.8	Species differences	12
2.9	Impaired ears	14
2.9.1	Histology	15
2.9.2	Correlations to physiological data	17
3	Characteristics of single-unit responses	19
3.1	Growth and temporal measures	19
3.2	Single-fiber responses to biphasic stimuli	23
3.3	Refractory effects	26
3.4	Channel interactions	27
3.5	Effects of stimulus polarity	28
4	Modeling studies	30
4.1	Phenomenological model of the EAP	30
4.2	Biophysical model of the auditory nerve: single units	33
4.3	Biophysical model of the auditory nerve: EAP	34
4.4	Manipulation of membrane noise properties	36
5	Human studies	37
6	Summary	39
7	Publications and patents	41

1 Introduction

Despite the substantial successes that have been demonstrated with cochlear implants, there are clearly limitations in the transfer of information to the central nervous system in individuals using these devices. We suggest that at least some of those limitations may be related to spatial and temporal interactions inherent in current cochlear implant designs. The research on this project was aimed at eventual development of alternative means of stimulating the auditory nerve. Our approach was to use computer simulations and experimental data to:

1. Characterize the fundamental spatial and temporal properties of intracochlear stimulation of the auditory nerve.
2. Evaluate the use of novel stimuli and electrode arrays.
3. Evaluate proposed enhancements in animals with partially degenerated auditory nerves.

In this document we present major findings obtained under Contract NIH N01-DC-6-2111. Sections 1 and 2 summarize our experience in recording the EAP and single unit responses to electrical stimulation in different animal species. Section 3 outlines model simulations of both single-unit and population response properties. Section 4 outlines preliminary results from animals with partially degenerated auditory nerves. Part of the work scope for this contract was to plan collaborations with groups working with auditory prosthesis users. We include preliminary results from human implant subjects in Section 5 to illustrate the applicability of our results to clinical populations. Section 6 is a summary. Finally, in Section 7 we list the publications and patent applications that have been completed during this contract period. This document provides a general overview of major findings; more detailed information can be found in several peer-reviewed publications listed in Section 7.

2 Characteristics of the EAP

2.1 Morphology and growth

We have performed extensive measures of the EAP in 17 cats and 11 guinea pigs using monopolar, monophasic stimuli. Our goal was to characterize response patterns with these relatively simple stimuli, to use the data to refine

characteristics of our neural models and to subsequently provide a basis for a better understanding of the response properties to more complex stimuli. These experiments have characterized responses across a range of stimulus levels, polarities, and durations. Response measures include latency, morphology, width, amplitude, growth rate, and conduction velocity. Because we used the same stimulus paradigms in both species, our measures were particularly suited for across-species comparisons.

Figure 1 illustrates waveforms, latency-level functions, and amplitude-level functions typical of data obtained from both guinea pigs and cats. The EAP has a stereotypic waveform occurring within 1 ms after stimulus onset, with a morphology that is dependent on stimulus polarity. In general, maximal response amplitudes are larger in the cat than in the guinea pig. With few exceptions, the amplitude-level (growth) function is monotonic, with the amplitude at EAP saturation unaffected by stimulus polarity or pulse duration. Cathodic latency was consistently longer than anodic latency in both species. In cats, thresholds were generally higher than those obtained from guinea pigs and cathodic threshold was lower than anodic. In contrast, the guinea pig preparations yielded anodic thresholds that were lower than cathodic thresholds. These results are published in Miller et al. (1998). Our model simulations are basically consistent with these measures. One exception is the species difference observed in the polarity-dependent threshold values. Anatomical differences between cat and guinea pig cochlea may be responsible for the unexpected polarity effects observed in the guinea pig thresholds. These results suggest that polarity-specific stimuli are important in assessing threshold and growth properties of electrical stimulation of the auditory nerve. The differences between cats and guinea pigs also underscore the possible importance that anatomical differences and electrode placement may have on the nerve excitation process.

We have also observed growth functions that are not as easily explained by model simulations in that the saturation amplitudes evoked by anodic stimuli are sometimes less than for cathodic stimuli. These amplitude differences can be consistently observed across pulse durations, as well as with changes in the stimulating electrode position (see Miller et al., 1998). Possible explanations of this effect include either polarity effects on the size of the recruited fiber population or on the size of the unitary potential (Kiang et al., 1976). Neither of these effects is predicted by physiologically “reasonable” modifications of our biophysical model. However, we note that we are unable to realistically address the spatial effects of intracochlear excitation fields at this time. As noted in Section 3, however, the significantly different

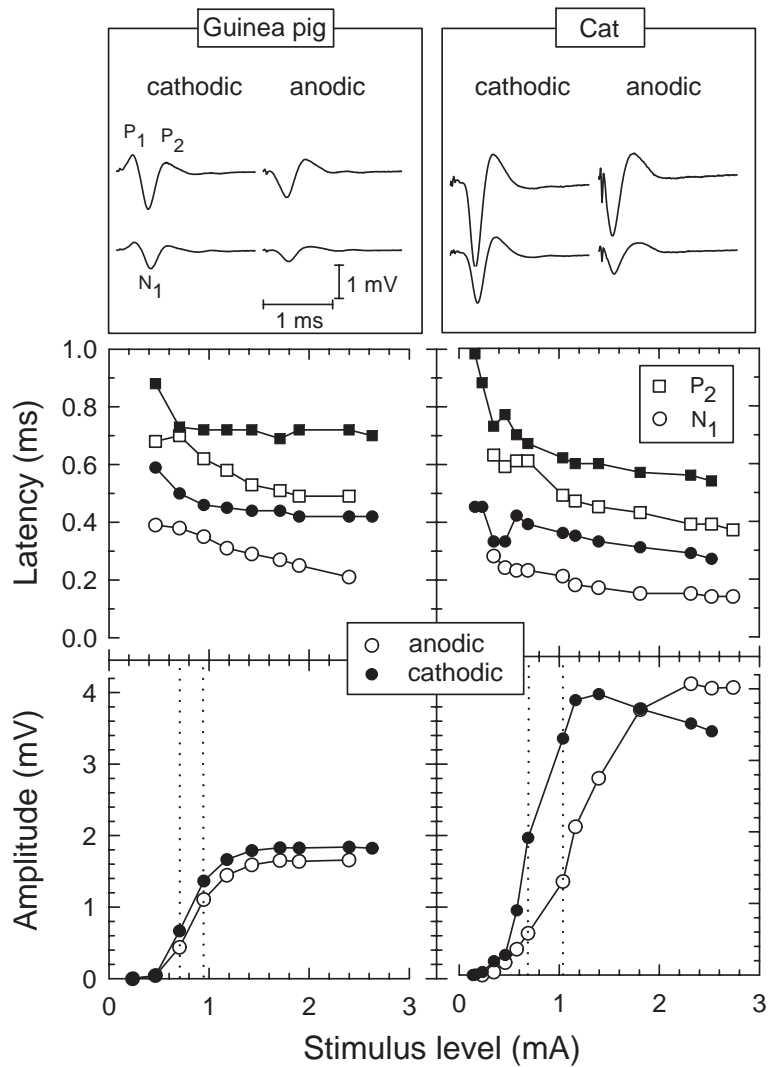


Figure 1: Examples of electrically evoked compound action potential (EAP) data from guinea pigs and cats obtained with monophasic stimuli delivered by a monopolar intracochlear electrode. Top panels illustrate typical EAP waveforms, while the middle and bottom panels show latency-level and amplitude-level functions, respectively, for both stimulus polarities.

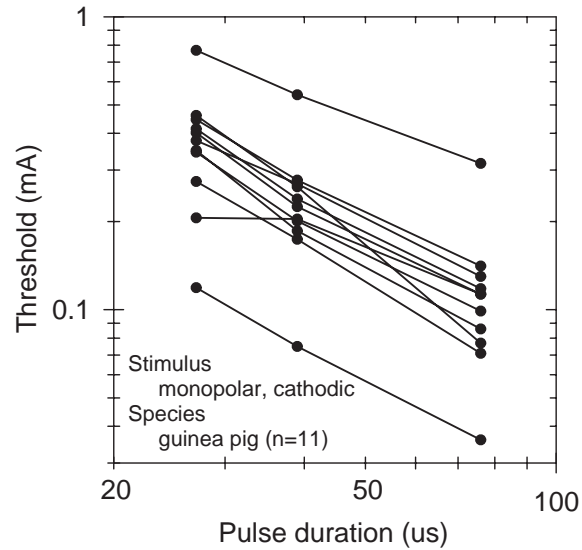


Figure 2: EAP strength-duration functions obtained from 11 guinea pigs. Monophasic cathodic stimulus pulses were delivered by a monopolar electrode positioned in the basal turn of the cochlea.

adaptation effects for cathodic and anodic stimulation observed in single unit data may also be factor in this observation.

2.2 Strength-duration function

The integration of current by an excitable membrane is often characterized by the strength-duration function (e.g., Hill, 1936; Bostock, 1983). We evaluated the strength-duration characteristics of both cat and guinea pig EAPs using monophasic stimuli delivered by a monopolar electrode (Miller et al., 1998). This “classic” mode of stimulus delivery is essential for success in interpreting data in terms of basic biophysical processes. Strength-duration data obtained from 11 guinea pigs with cathodic stimuli are shown in Figure 2. Further work at a single-fiber level is still needed in order to refine characteristics of the model as well as to develop a better understanding of integrative characteristics necessary to predict responses to more complex waveforms.

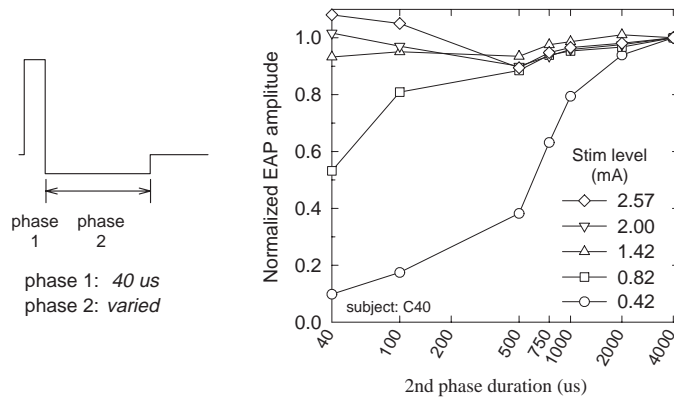


Figure 3: The effects of second phase duration of biphasic, cathodal-first, pseudomonophasic pulses on feline EAP amplitudes. In all cases, the duration of the first (cathodal) phase was fixed at $40 \mu s$ and the second phase duration was varied systematically. To facilitate comparisons, EAP amplitudes are normalized to the maximum amplitude evoked by a monophasic pulse.

2.3 Response to pseudomonophasic pulses

Pseudomonophasic pulses are charge-balanced pulses where the initial phase has a shorter duration than the second phase. As a result, when the second phase is relatively long in duration, these stimulus pulses are effectively monophasic. Such stimuli may be a useful alternative to biphasic pulses since they may provide greater control over neural excitation. To characterize the EAP in response to pseudomonophasic pulses, we fixed the first phase at $40 \mu s$ and varied the duration of the second phase. Figure 3 shows a series of EAP functions obtained from a cat. Response amplitude is plotted as function of second phase duration. At high stimulus levels there is relatively little dependence on second phase duration, but at low stimulus levels, the EAP amplitude is depressed over a wide range of second phase durations. Similar effects of second duration were obtained doing analogous experiments with single fibers (see Section 3).

2.4 Recovery of the EAP from forward masking

The stimulation through a cochlear implant is rarely in the form of a single pulse but rather as sequence of pulses which carries information relative to the stimulus waveform. One way in which prior stimulation may affect the response is through refractory properties of the nerve. We have in-

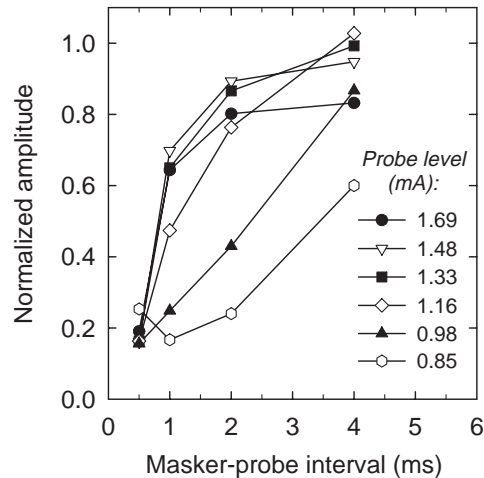


Figure 4: EAP forward-masking recovery curves. EAP amplitudes to a forward-masked stimulus are plotted as a function of masker-probe interval for several probe levels. In all cases, $40 \mu\text{s}$ cathodic pulses were used. Amplitudes are normalized to that produced by an unmasked stimulus.

investigated these properties of the EAP using a two-pulse (masker-prober forward masking paradigm). We typically examine the response to the probe as a function of the interpulse period (IPI) between the masker and probe pulses. Under most stimulus conditions, the response to the probe is fully recovered from masking for IPIs greater than 10 ms. Figure 4 shows typical amplitude recovery functions from a cat, with the level of the probe and masker varied parametrically. These data illustrate that the rate of EAP recovery from masking is dependent on the level of the probe: higher probe levels result in faster recovery. This trend is consistently observed in our animal data, as well as that from humans (Abbas et al., 1997b; Finley et al., 1997; Hong et al., 1998) and our model (Section 4.1). This observation underscores the importance of obtaining forward-masking data at several stimulus levels so as to fully characterize this property. We have also used single fiber recordings to better understand the basis of these level effects inherent in EAP measures (Section 3).

2.5 Channel interaction

One way in which to functionally assess spatial properties of intracochlear electrical stimulation is through the use of channel interaction measures

using the EAP. We have used cats as an experimental subject in these experiments thus far and have used a multi-electrode array supplied by Clarion Corp. similar to the array used in Smith et al., 1994. With this array we have typically used electrodes 1,2,4,6, and 8 which are placed on the modular side of the carrier and ordered from apex to base. Channel interactions can occur due to overlap in the electric stimulus fields as well as overlap in the stimulated neural populations. We have chosen to use a masker-probe stimulus paradigm in order to assess channel interaction. By using a forward masking paradigm (masker pulse on one electrode and a delayed stimulus pulse on a second electrode) simultaneous interactions of the electric field from each electrode are eliminated so that interactions that are observed should be solely from the overlap in the neural populations stimulated by each electrode. By measuring a peripheral response we can further limit our measures to interactions among auditory nerve fibers.

Spatial interaction measures involve a complex interaction of masker level, probe level and electrode placement. Since the sensitivity for each electrode in the array can be quite different we have chosen to normalize the probe and masker levels relative to the maximum amplitude elicited by each stimulus for that stimulating electrode. We can therefore specify level as percent of maximum EAP amplitude, i.e., the level corresponding to a certain amplitude of response normalized for that particular electrode's EAP growth function. The percent interaction is then calculated as the decrease in response to the probe with the masker present relative to the response to the probe alone. These normalizations enable us to report "effective" stimulus levels that account for differences in electrode sensitivity.

Figure 5 plots the percent interaction (i.e., normalized amplitude decrement) as a function of masker level (expressed in percent of maximum EAP amplitude). In all cases the masker pulse is presented on electrode 1. Data are plotted for several levels of probe (expressed in percent of maximum EAP amplitude) as well as for several probe electrodes. Two trends are evident in the data. First, they demonstrate a degree of spatial selectivity in that for a particular level of masker and probe the degree of interaction tends to decrease with increasing distance between probe and masker channels. The data also illustrate that this measure of interaction is highly dependent on the response amplitude to either the masker or probe; the interaction tends to increase with increasing masker level and to decrease with increasing probe level. The effects of level are particularly important in attempting to understand some of the issues addressed in Sections 2.8 and 3.4 regarding site of spike initiation and current level.

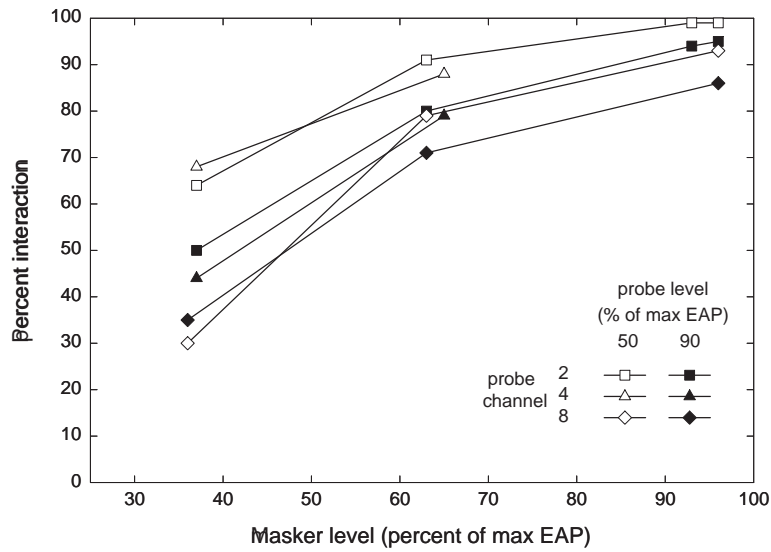


Figure 5: Stimulus electrode (channel) interaction assessed using an EAP forward masking paradigm in which masking and probe stimuli are presented to different intracochlear electrodes. Interaction is assessed by the degree to which the masker decreases the probe response relative to the unmasked condition. Both the abscissa and ordinate values are normalized to allow meaningful across-electrode comparisons. On the abscissa is plotted effective masker level; that is, level is expressed in terms of the corresponding masker response amplitude relative to maximum EAP amplitude for that electrode. On the ordinate is plotted percent interaction, defined as the decrease in response due to masking relative to the response amplitude of the unmasked probe. Plots are shown for three different probe electrodes and two different levels of the probe (indicated as percent of maximum EAP). In all cases the masker pulse was presented on electrode 1 and the IPI was 0.5 ms.

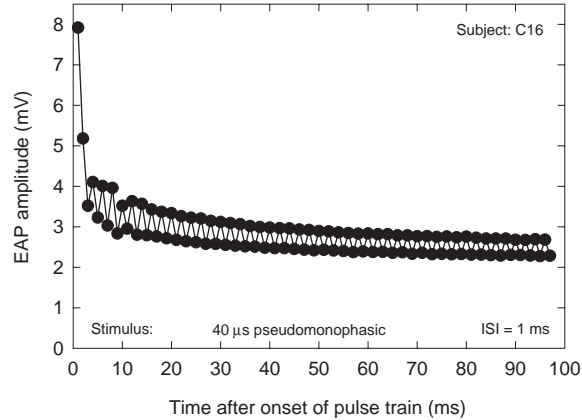


Figure 6: Plot of feline EAP response amplitudes to a series of constant-amplitude stimulus pulses of a pulse train. Both the alternation amplitude and average amplitude decrease over time.

2.6 EAP responses to pulse-trains

While refractory properties, as assessed with a two-pulse stimulus paradigm, can provide important information relative to the temporal interaction of pulsatile stimuli, the responses to longer sequences of stimuli may demonstrate more complex temporal interactions. As part of this research we have measured EAP responses to trains of electrical pulses (typically 100 ms in total duration) and have systematically examined the effects of stimulus amplitude and interpulse interval on the patterns of responses to these trains. We have also examined the effects of stimulus pulse shape on these patterns. Pseudomonophasic and biphasic pulse trains from both guinea pigs and cats evoke qualitatively similar response characteristics. Figure 6 shows a sequence of feline EAP amplitudes to a constant-amplitude pulse train. The amplitudes are normalized to that of the first pulse in the train. These data reveal refractory properties in that the response to the second pulse is smaller than that to the first pulse. In addition, the response to successive pulses shows an alternating pattern, as well as an overall decrease in response amplitude, likely the result of refractory recovery and cumulative adaptation effects, respectively. The amplitude of alternation is highly dependent upon the IPI value, with the greatest degree of alternation occurring at IPIs near 1 ms.

Response patterns that we have recorded from cats and guinea pigs are

also qualitatively similar to those from implant patients (Wilson et al. 1995; Wilson, 1997). We do, however, typically observe smaller amplitude alternations in our animal preparations. Also, these alternations appear to decay faster; in some animals, the pattern was evident for only 50 ms. These differences could be due to a number of factors. Stochastic properties of the stimulated neurons likely affect the alternation pattern. Higher noise levels in the neural membranes of recently deafened animals may result in more stochastic response patterns. In addition, anatomical differences and differences in placement of the stimulating electrode may affect site of activation. Finally, as described below, we have begun analysis of measures of pulse trains in ears with spiral ganglion cell depletion. Those results in comparison to neuron survival patterns may afford additional insight into the differences between experimental animals and humans.

The use of amplitude-modulated pulse trains brings us one step closer to a realistic simulation of CIS-like excitation of neurons. The plots in Figure 7 show amplitudes of EAPs in response to an amplitude-modulated pulse train. The depth of modulation was systematically varied in order to assess the modulation range over which the nerve faithfully encodes amplitude information. The data shown were obtained 150 ms after onset of the modulated pulse train so that an approximate steady state response was reached (that is, any onset effects have died out). Note that in the case of 0% modulation (i.e., constant amplitude pulse train) the response is constant. That is, any alternating pattern that may have been present in the response has completely decayed within the first 50 ms of stimulation. As modulation depth was increased, an approximately sinusoidal modulation of response amplitude emerged. At higher modulation depths the response pattern shows larger variations but becomes distorted.

A modulated pattern of response at relatively low modulation depths (as low as 1%) is typical of our data. The pattern of distortion has been analyzed using Fourier analysis of these response patterns; a distorted pattern is evident as shown at high modulation depths. Distortion tends to be greater at very low stimulus levels and at high stimulus levels. We have attributed this distortion to both nonlinear growth characteristics and refractory properties of stimulated neurons.

We have also measured the modulation of the response as a function of modulation frequency, at a fixed level and modulation depth. We consistently observed an increasing degree of response modulation with increasing modulation frequency, in one animal up to 1600 Hz. Such data suggest that the peripheral response to temporal modulation is robust even at frequencies

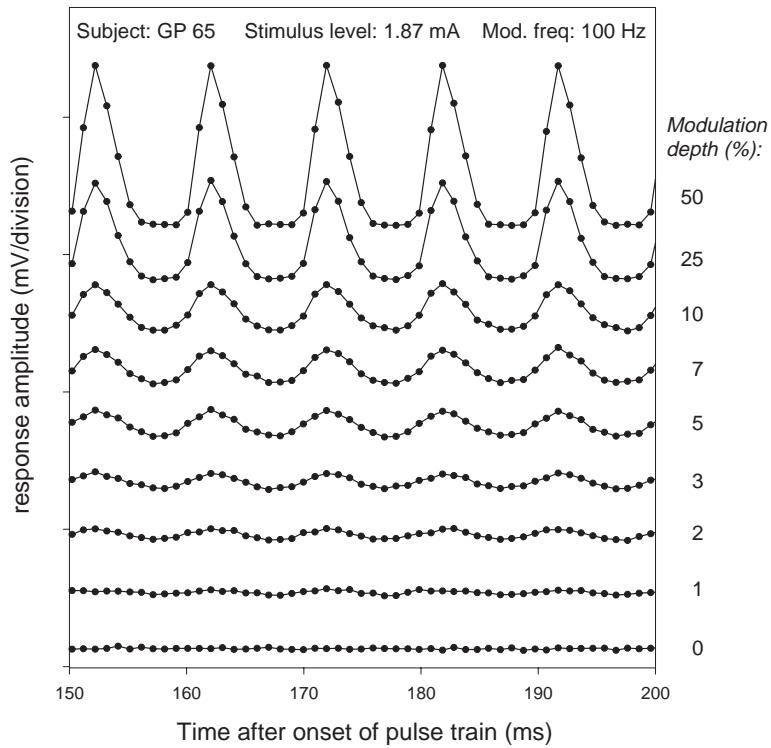


Figure 7: Plot of EAP amplitudes in response to a sinusoidally modulated pulse train. Data were obtained from a guinea pig stimulated with a monopolar intracochlear electrode. Biphasic pulses of $40 \mu\text{s}$ /phase duration were presented at a rate of 1 pulse per ms. Shown are several response patterns obtained at different modulation depths. Stimulus level of the unmodulated carrier was kept constant across conditions.

where modulation perception is not typically evident.

2.7 Conduction velocity estimate

Experimental measures of action potential conduction velocity would contribute to accurate models and predictions of responses from the auditory nerve. Figure 8 illustrates results from our first EAP measurements designed to estimate the conduction velocity of feline auditory nerve fibers. This experiment was conducted on a preparation that provided relatively generous exposure (up to 2 mm) of the length of the auditory nerve. The recording ball electrode was placed at five different positions along the length of the nerve (as measured by a micrometer stage) and EAP growth functions measured at each position. The amplitude for both anodic and cathodic stimulation varied across recording position but the waveforms for all five recording positions showed clear N1 and P2 peaks. As expected, the latency of the peaks varied with medial-to-lateral recording positions.

Calculated conduction velocities based on these measures are plotted in Figure 8. Conduction velocities were calculated only on the basis of latency differences obtained at the extreme ends of the five recording sites shown in the figure. Separate estimates of conduction velocity were made using the N1 and P2 peaks of the EAP. The figure shows that estimates based on these two peaks yielded slightly different, but generally overlapping, values of conduction velocity. The mean values plotted across all estimates for this animal yield values ranging from 14 to 17 m/s. Anatomical surveys have estimated the diameter of the myelinated central axons to be between 2 and 4 microns (Arnesen and Osen, 1978; Liberman and Oliver, 1984). Estimates of conduction velocity based upon fiber diameter (Hursh, 1939; Burgess and Perl, 1973) yield velocities consistent with this preliminary estimate.

2.8 Species differences

While the single-fiber data has been limited to measures on cats, we have made extensive measurements of the EAP on both cats and guinea pigs. Since the cochleae of the cat and guinea pig are somewhat different anatomically, these measurements afford the opportunity to evaluate the extent to which such anatomical differences may affect the physiological responses. In general, the responses are quite similar between the two species. Morphology of responses, latency differences with stimulus polarity, and other basic properties of the response are similar. Several differences in response

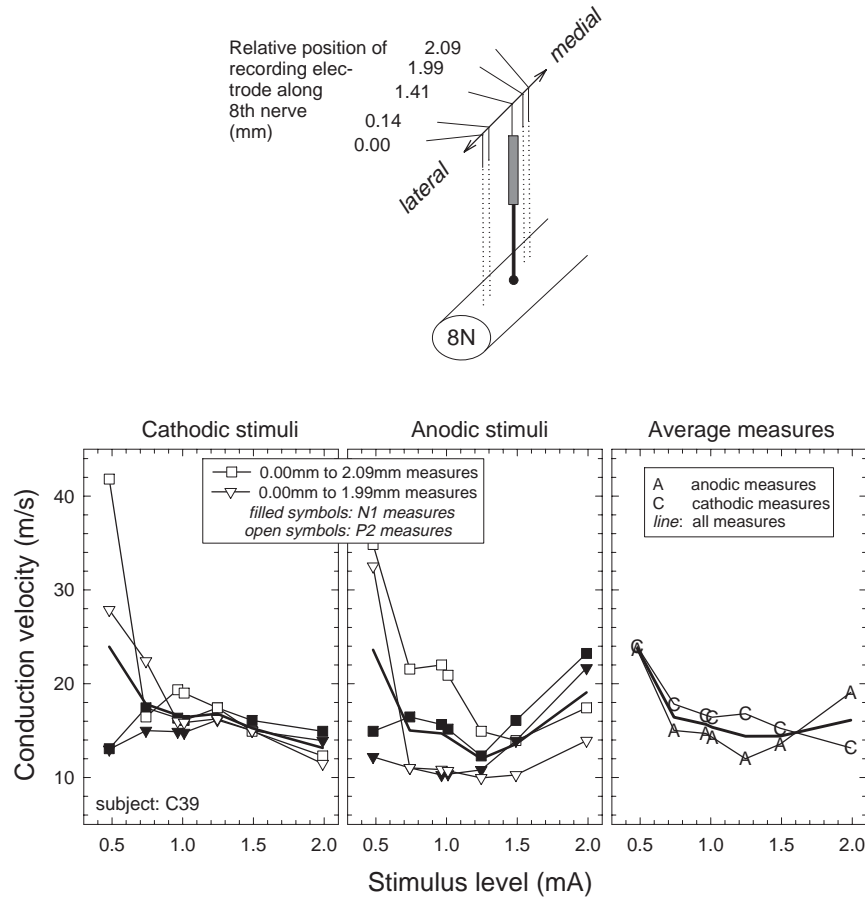


Figure 8: Preliminary estimates of auditory nerve conduction velocity. All estimates are shown plotted as functions of stimulus level. Various estimates are shown for both cathodic (left panel) and anodic (middle panel) stimuli. Both the latencies of the N1 and P2 peaks were used and are plotted separately by filled and open symbols, respectively. Two sets of repeated measures were obtained by recording EAP input-output functions at a total of three different sites, as indicated in the legend. The graph of the right panel plots the average anodic, average cathodic, and overall average measures of conduction velocity.

to basic stimuli have been described in some detail in Miller et al. (1998). For instance, with cats the difference in threshold for anodic and cathodic stimuli are consistent with a model of monopolar activation in a uniform medium. In guinea pigs the threshold difference is in the opposite direction, i.e., anodic thresholds tend to be lower than cathodic thresholds. The data with pulse trains also has demonstrated differences in the temporal response properties between the two species. Guinea pigs generally produce a relatively larger alternating pattern in response to constant amplitude pulse trains (Matsuoka et al., 1998). Guinea pigs also do not show consistent differences with stimulus polarity as described above for cats.

The most salient anatomical difference between the cat and guinea pig cochlea is the more compact spiral in the guinea pig which results in the basal stimulating electrode being closer to the modiolus. In both species, the specialized structures such as the unmyelinated dendrite and cell body may have an effect on the neuronal response properties to electrical stimulation. If the stimulation site is close to those structures, one may expect particularly large effect on membrane time constants and consequently on refractory properties and adaptation. We hypothesize that in cats, the stimulation site may be more peripheral than in guinea pigs where the stimulating electrode is closer to the modiolus. The resulting current paths would be quite different for the two species and the effects of the peripheral structures may be greater in the cat resulting in different temporal properties. This hypothesis is also at least consistent with the observed differences in response alternation with pulse trains. The "noisier" dendrites may reduce the alternation pattern in cats where the spike initiation site is nearer.

2.9 Impaired ears

Most measurements reported on up to this point have been with animals which are acutely deafened, presumably leaving a relatively intact neuronal population but no functional hair cells. This animal model provides a best case response, but humans who typically receive cochlear implants likely have significant neuronal degeneration. The degree to which these observations are valid and/or different in animals with neural degeneration is consequently an important consideration for potential applications of these data to human subject populations.

2.9.1 Histology

We have conducted experiments on a series of 20 guinea pigs which have been deafened and then allowed to survive for 4 to 16 weeks in order to effect varying degrees of neural degeneration. We have used both exposure to noise (115-120 dB for two hours) or injections of kanamycin (400 mg/kg) and ethacrynic acid (40 mg/kg) to reduce hair cell populations and consequently result in neural degeneration. After the survival period, each animal underwent the same procedure for recording as normal animals in these experiments. Recordings of responses to single pulses, pulse trains, and in some cases modulated pulse trains were evaluated. After data collection each animal was perfused and the cochleae prepared for histological analysis. Cell density measures of spiral ganglion populations were made using a point-counting procedure similar to that described by Weibel (1979). While samples across the entire cochlea will be analyzed, to date we have only cell density (percent cell volume) for a section 3-3.5 mm from the base of the cochlea. This location was chosen for initial analysis since it is just basal to the placement of the stimulating electrode and typically does not demonstrate damage that can arise from electrode insertion. Data from 18 animals are discussed in this section.

The histological analysis showed a range of cell loss in these experimental animals. Examples of a cochleae section from two animals which underwent kanamycin/ethacrynic acid injection (Panel A and B) and one untreated animal (Panel C) are shown in Figure 9. The cell depletion is evident in both experimentally treated animals. The cell volume (at a point 3.0-3.5 mm from the base) ranged from 2.06 to 36% (normal range 25-35%) for the subgroup of 18 animals analyzed thus far. These analyses demonstrate that we have successfully created a range of spiral ganglion cell depletion in these guinea pigs. Our initial analyses, presented here, compares this group with the group of untreated animals for which we have extensive physiological data. It should be noted in these comparisons that both groups are treated at the time of the experiment with neomycin in order to eliminate hair cell activity. Thus neither group should have functional hair cells. The normal group should have no significant neural degeneration while the experimental group has demonstrated varying degrees of spiral ganglion cell loss. Preliminary assessments of correlations between responses and histology within the treated group are presented; further analyses with more complete cell density measures will likely be more productive.

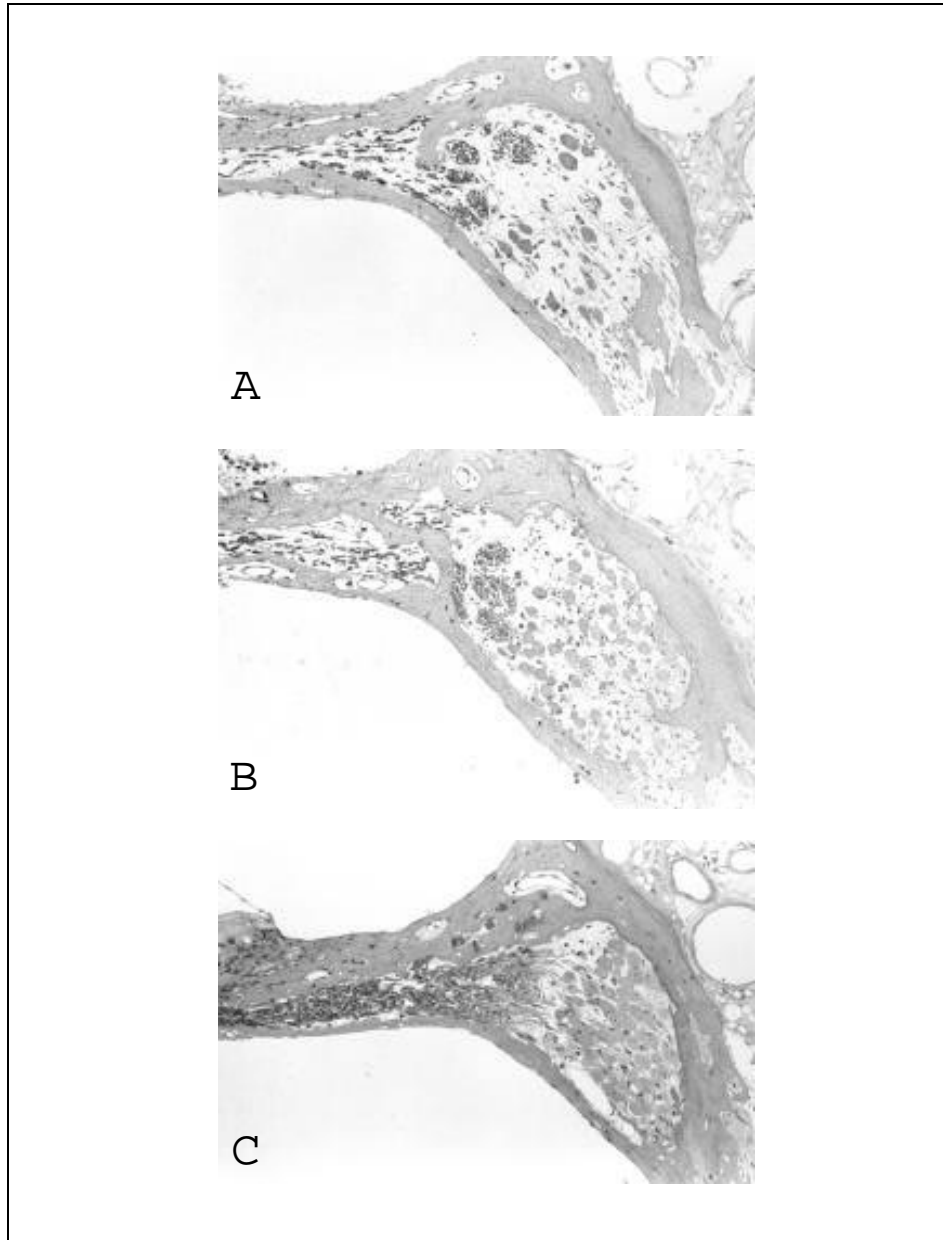


Figure 9: Histological sections of showing spiral ganglion cell survival in the cochlea of 3 animals. Panels A and B show section from animals deafened with ethacrynic acid and kanamycin. Panel C shows a section from an untreated animal. In all cases sections were taken approximately 3 mm from the cochlear base, close to the placement of the stimulating electrode.

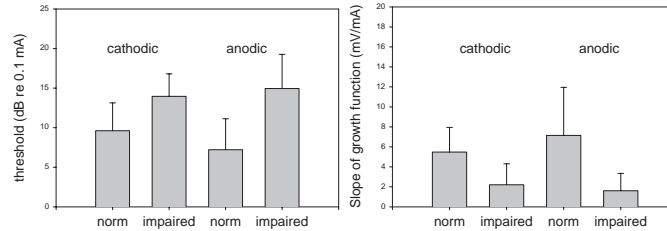


Figure 10: Comparison of EAP measures obtained from “normal” and “impaired” guinea pigs. “Normal” guinea pigs (n=10) were deafened by local application of neomycin at the time of data collection; “impaired” (n=12) were chronically deafened (by either noise exposure or kanamycin / ethacrynic acid administration) and allowed to survive several weeks prior to data collection. This group, too, was also given neomycin treatment at the time of data collection. The left panel shows a comparison of EAP threshold (defined by a response amplitude of $100 \mu\text{V}$) for these two groups for both anodic and cathodic $40 \mu\text{s}$ monophasic stimulus pulses. The right panel shows a similar comparison for the maximum slope of each subject’s EAP amplitude- level function. The effects of chronic deafening are observed in both the threshold and slope measures for both stimulus polarities.

2.9.2 Correlations to physiological data

Figure 10 compares the basic measures of threshold and growth of the EAP for a group of normal subjects reported on in Miller et al. (1998) compared to the group of subjects with depleted spiral ganglion cell populations. Note that for both cathodic and anodic stimulation, thresholds tend to be higher in the impaired group and the slope of the growth function tends to be lower. These data are consistent with our own previous work with the brainstem response (Miller et al., 1994) as well as that of others (Hall, 1990; Smith and Simmons, 1983). Data examining the correlation between these two physiological variables and spiral ganglion cell survival within the experimental group are plotted in Figure 11. In this case, data are plotted for both monophasic and biphasic pulses. While the data show considerable scatter, there is a trend for increased threshold and decreased slope with increasing spiral ganglion cell survival. The scatter in these plots is of interest in light of the discussion in Section 2.8 relative to the possible sites of nerve activation in the guinea pig. If neural activation occurred primarily within the modiolus in these preparations, then neuron survival at the electrode site may not correlate best with physiological data. After further histological analysis is conducted, we will re- evaluate these correlations.

At this point we have collected relatively little data with pseu domono-

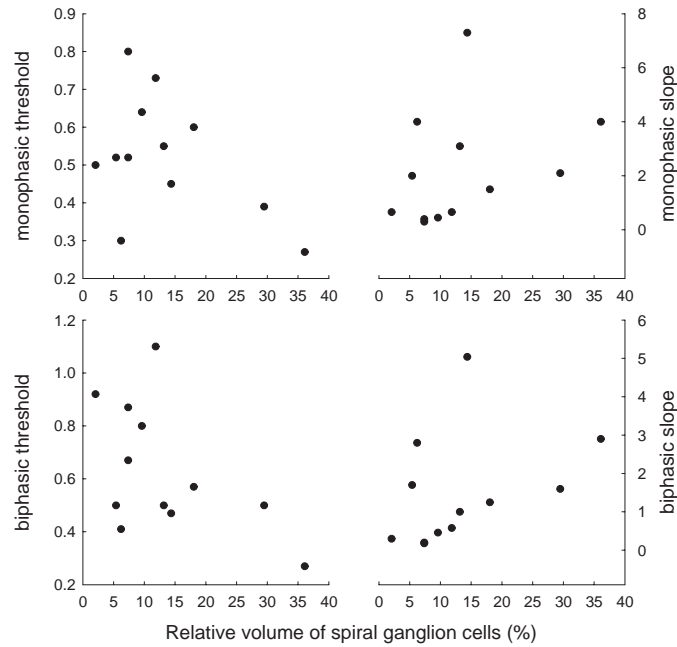


Figure 11: Preliminary analysis of possible correlations between electrophysiological measures and histological assays obtained from chronically deafened guinea pigs. Each datum represents a chronically deafened guinea pig. On the ordinates are plotted threshold and slope measures obtained using cathodic monophasic (top graphs) or cathodic-first biphasic (bottom graphs) stimuli. These measures are defined in the same manner as in Figure 10. The relative volume index indicates the percentage of cross-sectional area of Rosenthal's canal occupied by spiral ganglion cell bodies. Thus, with neural degeneration, relative volume decreases as fewer cell bodies occupy the canal.

phasic pulse trains in this population. By measuring the response amplitude as a function of second-phase duration, we can evaluate the degree to which the second phase affects the amplitude of response (as discussed in Section 2.3). The decrease in response amplitude is used to assess the degree of nerve-membrane integration. Figure 12 plots response amplitude at a fixed second phase duration as a function of stimulus level. In order to better compare data across animals with different sensitivities we have plotted stimulus level in terms of the equivalent response to a monophasic stimulus. Across the range of stimulus levels, the normalized EAP amplitude is greater for the animal with relatively normal spiral ganglion cell volume and depressed for those animals with spiral ganglion cell depletion. While this analysis is clearly preliminary, it suggests that the effect of second phase duration may be exaggerated in depleted populations, possibly due to changes in the membrane characteristics of neural populations or in the primary site of spike initiation.

Data on both constant-amplitude and amplitude-modulated pulse trains have been collected in animals with depleted neural populations. The normative response characteristics described in Section 2.6 such as response alternation, modulation of response and distortion were evident in the data from impaired animals. Preliminary analyses comparing quantitative assessments of these parameters have not shown any clear trends related to cell survival. Nevertheless, as we complete our histological analyses, we will re-evaluate these data.

3 Characteristics of single-unit responses

The measurements that we have conducted with the EAP allow us to characterize responses over a wide range of stimulus conditions. The EAP has inherent limitations in that the response is dependent on a population of neurons which may have different sensitivity and response characteristics. In order to better characterize both the response properties of single fibers and also the relationship between EAP and single fiber responses, we have made single fiber measures on a subset of the stimulus conditions for which we have made EAP measures.

3.1 Growth and temporal measures

Single-fiber data were obtained from 257 fibers of 14 cats (Miller et al., 1999a). Exemplar spike waveforms and basic analyses are depicted in Fig-

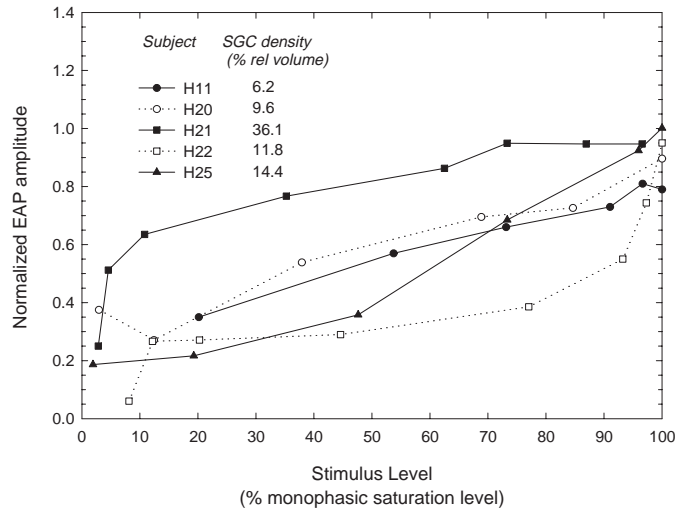


Figure 12: Normalized EAP amplitude-level functions for five guinea pigs with various degrees of spiral ganglion degeneration. EAP amplitudes and stimulus levels are both normalized to the saturated monophasic response to facilitate across-animal comparisons. Functions were obtained using cathodic- first “pseudomonophasic” pulses with a $40 \mu s$ initial phase duration and a second phase duration of $100 \mu s$. With a second phase duration of $100 \mu s$, large current-integration effects were observed (c.f. Figure 3). With data plotted as shown, a low-sloped function is consistent with a relatively long integration time constant. Note that the function for the subject with an intact spiral ganglion population (subject H21) increases at a relatively fast rate, whereas the other functions increase more slowly over a wider range of stimulus levels.

Table 1: Summary of single-fiber characteristics obtained from acute cat preparations using monopolar, monophasic stimuli.

		26.8 μ s stimulus		39.0 μ s stimulus	
		cathodic	anodic	cathodic	anodic
Threshold (dB re 1mA)	mean	-0.88	1.0	-5.31	-2.72
	std dev	2.99	3.64	4.80	4.40
	n	94	55	148	91
Mean Latency at 50% FE (ms)	mean	0.606	0.440	0.647	0.456
	std dev	0.113	0.090	0.142	0.103
	n	90	49	146	91
Jitter at 50% FE (ms)	mean	0.0708	0.0619	0.107	0.0725
	std dev	0.0317	0.043	0.0866	0.0583
	n	85	44	146	91
Relative Spread	mean	0.0635	0.0618	0.0628	0.074
	std dev	0.0326	0.0404	0.044	0.073
	n	68	38	140	91

ure 13. After removal of stimulus artifact and waveform filtering, PST histograms were constructed and input-output functions obtained. These histograms provide measures of threshold, latency, jitter (standard deviation of latency), and relative spread. This latter measure, RS, is the normalized standard deviation of an integrated gaussian fit to the I/O function (Verveen, 1961); it is approximately proportional to the slope of the I/O function. Population data for these measures are given in Table 1.

Consistent with the cat EAP data, single-fiber cathodic latency and threshold are typically longer and lower, respectively, when compared to responses evoked by anodic stimuli. In a minority of units, cathodic threshold was higher. Rarely was cathodic latency shorter. These findings are again consistent with predictions of our biophysical model. The lower anodic thresholds seen in the minority of cases is consistent with differing orientations of the fiber terminal relative to the stimulating electrode (Rubinstein, 1993). Detailed quantitative analysis of RS, jitter and latency (Miller et al., 1999a) suggests that a minority of fibers, i.e., those serving the basal cochlea near the electrode, are activated at sites peripheral to the cell body by a cathodic stimulus. It is our interpretation that most fibers are activated central to the cell body, with the cathodic site more periph-

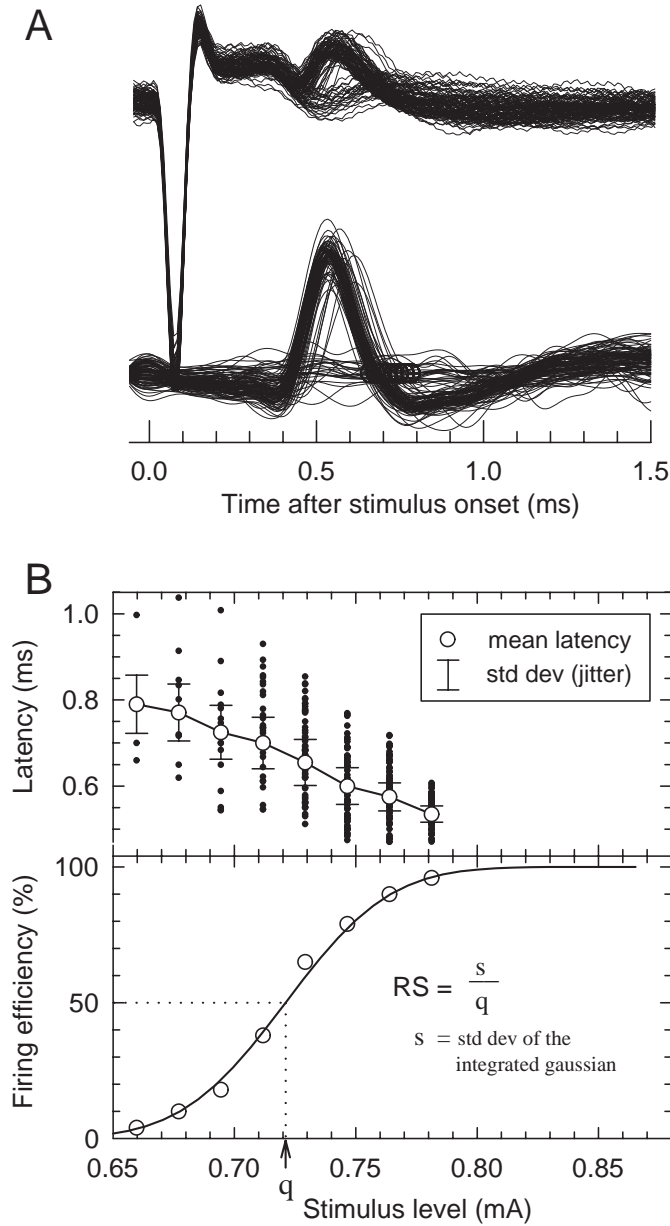


Figure 13: Exemplar single-fiber action potentials (top panel) and basic input-output functions (lower panels) typically obtained from single fibers from the electrically stimulated cat auditory nerve. We usually presented the fiber with 100 repeated stimuli in order to obtain estimates of mean latency (measured from spike peak), jitter, and firing efficiency (i.e. firing probability). The bottom plot illustrates an FE-level curve obtained by stimulating the fiber at several levels. Shown fitted to this data is an integrated gaussian function used to estimate Relative Spread (Verveen, 1961). Relative Spread is the normalized standard deviation of this gaussian function.

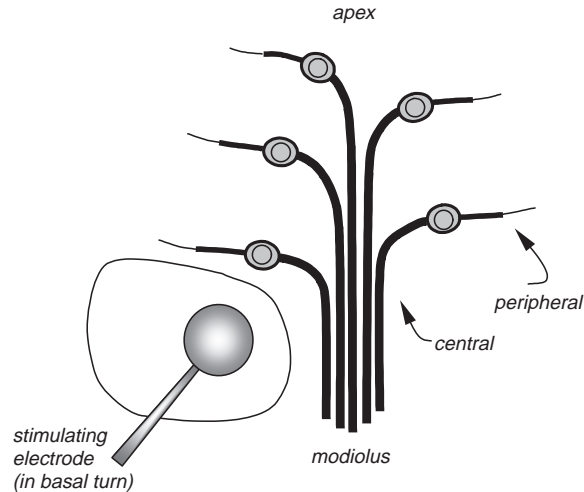


Figure 14: Schematized drawing of a mid-modiolar cross-section of a cochlea, with a monopolar stimulating electrode positioned in the basal turn. The myelinated central and unmyelinated peripheral processes are labeled.

eral than the anodic site. This conceptualization is reasonable in light of cochlear anatomy and the position of the stimulating electrode, as shown in the schematic drawing in Figure 14.

Only a small number of fibers (six fibers in four cats) yielded bimodal PST histograms, suggesting a discrete jump in site of excitation with increasing level of monophasic stimulation, as illustrated in Figure 15. Some fibers demonstrate this phenomenon with cathodic and some with anodic stimuli. Assuming that excitation site correlates with latency, the two discrete activation sites straddled the site associated with the opposite polarity in both fibers as shown in Figure 15. We speculate that these units were oriented so as to allow excitation sites straddling the cell body. However, the histograms are also consistent with complex activating functions (Rattay, 1989) due to atypical fiber orientations (Rubinstein, 1993).

3.2 Single-fiber responses to biphasic stimuli

Although bimodal PST histograms have been previously reported (Javel et al., 1987; van den Honert and Stypulkowski, 1987; Javel 1990), they were only evoked with biphasic stimuli, each phase of which can elicit spikes (van den Honert and Stypulkowski, 1987). A within-fiber comparison of response

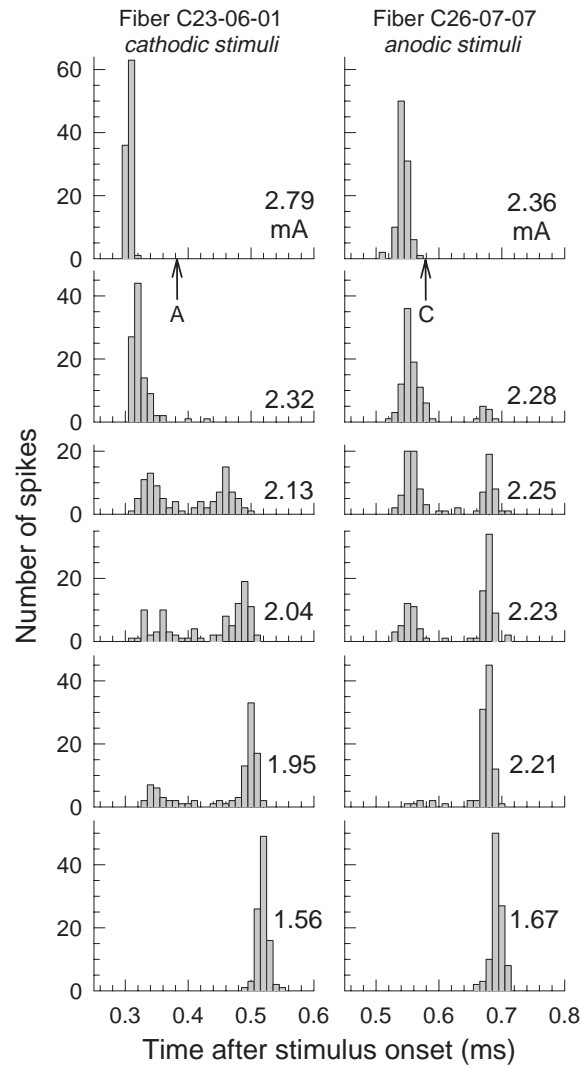


Figure 15: Post-stimulus time histograms of two fibers from two cats exhibiting level-dependent, bimodal distributions. In both cases, $39 \mu\text{s}$ monophasic stimuli were presented a total of 100 times. In all cases shown, the fibers responded at a firing efficiency of 100%. Stimulus level (in mA) is indicated as parameter in each graph. The arrows labeled "A" and "C" denote the mean latencies obtained for high level anodic and cathodic stimuli, respectively and allow for across-polarity comparisons of spike latency.

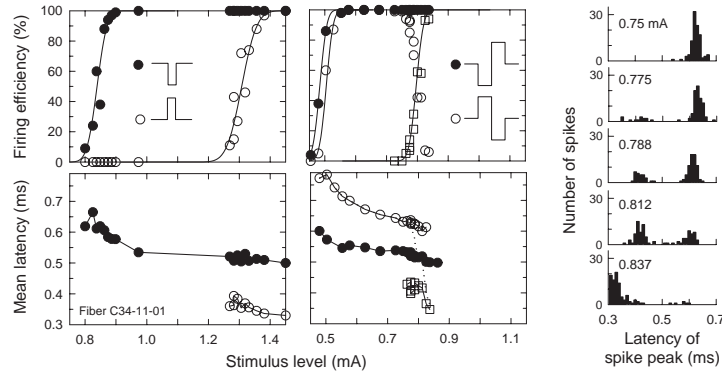


Figure 16: Input-output functions for a single cat auditory nerve fiber obtained with monophasic (left column) and biphasic (middle column) current pulses. With monophasic stimuli, cathodic pulses produced lower thresholds and longer latencies characteristic of our data. Biphasic stimuli produced complex response patterns, as described in the text. The histograms of the right column illustrate the bimodal response patterns that resulted with anodic-first biphasic pulses (open symbols).

patterns evoked with monophasic and biphasic stimuli is shown for one fiber in Figure 16. The left panels show FE-level and latency-level functions typical for $40 \mu\text{s}$ cathodic and anodic monophasic pulses. The middle panels show corresponding functions for $100 \mu\text{s}/\text{phase}$ biphasic pulses; note that the anodic-first biphasic pulses produced bimodal histograms (panels at the right). Several interesting comparisons can be made. First, note that the cathodic-first biphasic pulses produce a latency function very similar to that produced by the monophasic cathodic pulses. Over a stimulus range from 0.5 to 0.8 mA, the anodic-first biphasic pulses produced a latency function (lower middle panel) roughly parallel to the cathodic-first function, only shifted up by about $100 \mu\text{s}$. Once the fiber shifts to the earlier latency mode (at about 0.8 mA), the latencies correspond closely to those produced by anodic monophasic pulses.

These data illustrate the importance of examining responses with monophasic stimulation, even if that is not the modality typically used in cochlear implants and many research protocols. The potentially complex responses to biphasic stimuli are relatively difficult to interpret, given the potential for multiple excitation modes even with simple monophasic stimuli.

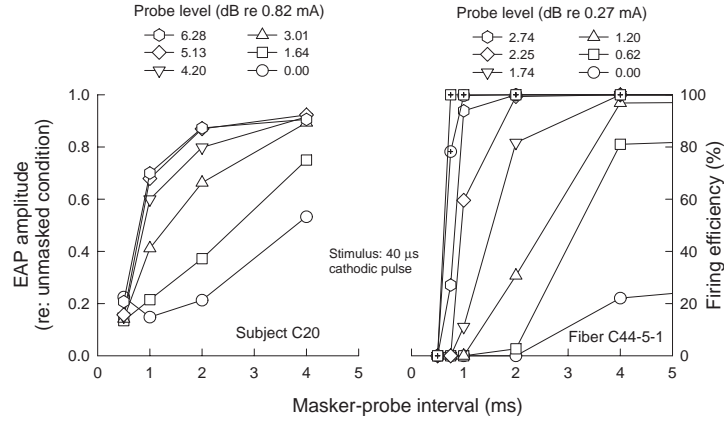


Figure 17: Refractory recovery functions for both EAP and single fiber measures in the cat. On the left, EAP amplitude, normalized to the unmasked response amplitude, is plotted as a function of interpulse interval. On the right, firing efficiency for a single fiber is plotted as a function of interpulse interval. Probe level is the parameter in both plots and is indicated in the legend.

3.3 Refractory effects

Refractory effects have been evaluated using a two-pulse stimulus and evaluating the response to the second pulse. The same paradigm has been used to evaluate both EAP and single-fiber responses. Figure 17 plots refractory recovery data for a single auditory nerve fiber (on the right) with a plot of EAP recovery for comparison. In both cases the recovery is measured for several stimulus levels, but there are several important differences in the response patterns. First, the effect of level on single fiber recovery occurs over a narrower range. Second, the single fiber recovery at high levels is much faster than that for the EAP. Complete firing efficiency recovery can occur for intervals as short as 750μ s. Furthermore, we estimate that the absolute refractory period is substantially less than 0.5 ms. We have attempted to reconcile these differences between single fiber and EAP response recovery in the discussion relative to EAP modeling (Section 4.1) below.

In addition to changes in the probability of action potential generation during the refractory period, we have also observed significant changes in action potential amplitude. Figure 18 illustrates response traces to 100 masker-probe stimuli. The masker pulses cannot be seen in these traces due to the template subtraction scheme that we have utilized to reduce probe artifact. What remains in this figure is one unmasked action potential and

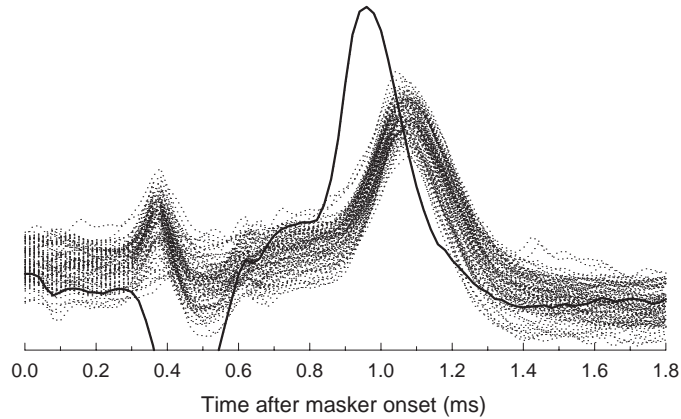


Figure 18: Single-fiber action potentials in response to the second pulse of a two-pulse stimulus. Recorded potential is plotted for 100 stimulus presentations. Masker pulse and action potential are subtracted out in the procedure used to eliminate probe artifact. In this series of stimuli, the dotted curves all demonstrated an action potential from the masker. The solid curve was the lone case in which the masker did not elicit an action potential. The action potential resulting from the probe is clearly larger in amplitude and earlier in latency than the 99 action potentials occurring after a masker action potential, during the relative refractory period.

many action potentials that have occurred after a response to the masker pulse. In all but one case, the masker pulse elicited an action potential. We observe a clear shift in the latency of the masked action potentials along with a reduction in amplitude compared to the unmasked spike. As outlined in Section 4.1, we propose that such changes in amplitude of the action potentials may be an important factor in the generation of EAP under similar stimulus conditions.

3.4 Channel interactions

Single-fiber input-output functions obtained with a USCF-type, multi-contact intracochlear array are shown in Figure 19. This array was designed to fit into the basal turn of the cat cochlea. In this experiment, four of the array's electrodes were used in monopolar configurations to stimulate single fibers. The longitudinal distance between each of the four chosen electrodes (designated 2, 4, 6, and 8 in the figure) is approximately 1 mm, with electrode 2 the most apical of the four. While these results are preliminary,

they are consistent with those of Hartmann & Klinke (1990) and some interesting trends are noted. Clear differences in sensitivity across stimulating electrodes are demonstrated, suggesting that a degree of channel independence. In at least two data sets of the fibers shown, there is greater independence among electrodes with cathodic stimulation. More importantly, the most sensitive stimulating electrode varies across fibers, consistent with a hypothesis of “place” selectivity for each stimulating electrode. In some cases, the ordering of electrodes for sensitivity varies with stimulus polarity. We have not as yet seen any systematic change in single-fiber RS values as a function of stimulus electrode.

3.5 Effects of stimulus polarity

One of the original goals of this research was to examine the basic properties of the neural excitation process in the cochlea with relatively simple stimuli. By using monopolar, monophasic stimulation and outlining the response properties both at the single fiber and whole-nerve level, we hoped to use that data to refine our biophysical neural model and consequently provide a better understanding to more complex stimuli. Both EAP and single fiber responses have demonstrated consistent differences with stimulus polarity. The EAP and single fiber responses have demonstrated a longer response latency to cathodic stimuli. As a result of this longer latency, the EAP can have a different morphology in response to anodic stimuli, showing an initial positive peak not typically seen with cathodic stimulation. In cats, both the EAP and single-fiber thresholds tend to be lower for cathodic stimulation; the trend is opposite for guinea pigs. When the EAP growth function is normalized to threshold, slopes for both cats and guinea pigs tend to be greater for cathodic stimulation than for anodic stimulation.

Many of these measures are highly dependent on stimulus level, but all observations are consistent with a more peripheral site of stimulation for cathodic stimuli. In addition, the single fiber data that we have collected to date show relatively few fiber (2%) which show evidence of bimodal histograms. The observation of bimodal histograms is consistent with the hypothesis of fibers being stimulated both peripheral and central to the cell body. These observations in conjunction with the differences observed with polarity suggest that relatively few fibers are stimulated at their peripheral process (possibly those near the stimulating electrode), while most are stimulated more central to the cell body. Nevertheless, most fibers are stimulated at different sites for anodic and cathodic stimuli.

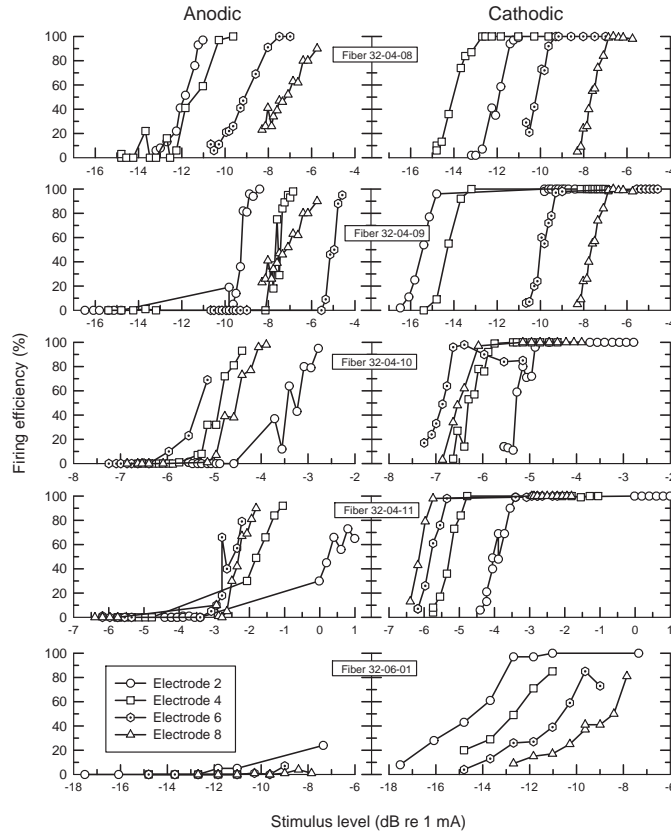


Figure 19: Input-output functions for five cat fibers obtained using the UCSF-type intracochlear array. Four electrodes of this array were used to stimulate at four different longitudinal sites. Electrode 2 is the most apical electrode; electrode 8, the most basal. Monophasic anodic (left panels) and cathodic (right panels) stimuli were delivered with each electrode serving as a monopolar source. Note that different decibel scales are used across fibers.

Data examining temporal measures are consistent with these observations in that there are also differences between the responses to cathodic and anodic stimuli, presumably due to differences in membrane and conduction properties and the site of spike initiation. Our data in cats using pulse trains have demonstrated a difference in the time course of adaptation across the pulse train in that anodic stimuli show a faster decrease to a similar steady state response amplitude as compared to cathodic. Similarly there are differences in the degree of response alternation in that cathodic stimulation can show maximum alternation at longer interpulse intervals (approximately 2 ms) than is typically observed with anodic stimulation (< 1 ms). In addition, our measures of single fiber response have demonstrated a relatively greater long-term adaptation with anodic stimuli. In some fibers the shift in sensitivity for anodic stimuli could be as much as 4-5 dB. These properties, in conjunction with the previous observations, suggest that temporal response properties — both short and long- term — may be affected by the site of stimulation. Furthermore, the relatively large shifts in sensitivity observed for anodic stimulation raises important questions regarding the interpretation of EAP measures using biphasic and/or alternating phase stimulation as well as the appropriateness of anodic stimulation for use in cochlear implants. Given the adaptation effects observed with anodic stimuli, such stimuli may not always provide stable responses or percepts in patients.

4 Modeling studies

4.1 Phenomenological model of the EAP

The relationship between electrically evoked single-fiber potentials and the EAP is part of the focus of our modeling work. Further development of our biophysical model is simplified by a quantitative understanding of the contribution of single fibers to the whole- nerve potential. This is also of obvious relevance to the interpretation of potentials that can now be recorded from humans with cochlear implants that feature EAP telemetry. A phenomenological model was developed based on the response characteristics of 230 fibers in 13 cats (Miller et al., 1999b). The fibers were stimulated by a brief monophasic pulse and PST histograms were pooled from 5000 modeled fibers to form a “compound” PST histogram. The compound histogram was then convolved with an estimate of the unitary potential to calculate the EAP using techniques described by others (Goldstein and Kiang, 1958;

Wang and Kiang, 1978; Wang, 1979).

This calculated EAP, as shown in Figure 20, could be manipulated by removal of the stochastic properties of jitter and RS from the modeled fibers. Such manipulations suggest that for single pulses, fiber threshold distribution is the primary determinant of the shape of the EAP growth function. We have also shown that if the fiber threshold distribution is significantly altered (i.e., compressed), then fiber properties of jitter and RS have a larger contribution to the growth of the EAP. Such compression may be present in the impaired ear. These fiber property manipulations - and their effect on model responses - are discussed in detail in Miller et al., 1999b). These results suggest that the observed threshold distribution of single neurons incorporated into the model dictates many of the properties of the EAP.

We have also used this model in a preliminary fashion to better understand other EAP response properties. For instance, the data presented in Section 2.3 on responses to pseudomonophasic pulses can be simulated using this model. Since the dynamic range of each single neuron is much smaller than the dynamic range of the EAP, as we increase stimulus level, fibers with low threshold will reach saturation. As a result, at low stimulus levels the properties of the EAP should be more similar to those of single fibers. At high levels, the majority of neurons are saturated and therefore the response reflects the saturated properties of the underlying single neuron responses. This prediction is substantiated by our direct comparison of experimentally-obtained single fiber and EAP data. Shown in Figure 21 are single fiber FE (left panel) and EAP amplitude data as a function of the second phase duration of a pseudomonophasic pulse. This comparison is consistent with the hypothesis that low-level EAP responses better reflect the underlying single fiber behavior.

Similar model analysis has been performed with two-pulse refractory paradigms such as those presented in Figures 4 and 18. In this case, the very fast recovery observed in single fiber responses predicts a similar fast recovery of the modeled EAP at stimulus levels, as shown in Figure 22. Note that for both the model (left panel) and experimental data (right panel), stimulus level is expressed relative to saturation level. EAP data from several animals demonstrates that the measured EAP shows a level effect but never demonstrates the relatively fast recovery evident in the model based on single fiber responses. It is important to note that the model only simulated reductions in firing efficiency; apparently this component alone does not adequately model the EAP recovery data. In our somewhat preliminary analysis we have investigated other parameters which may affect the EAP

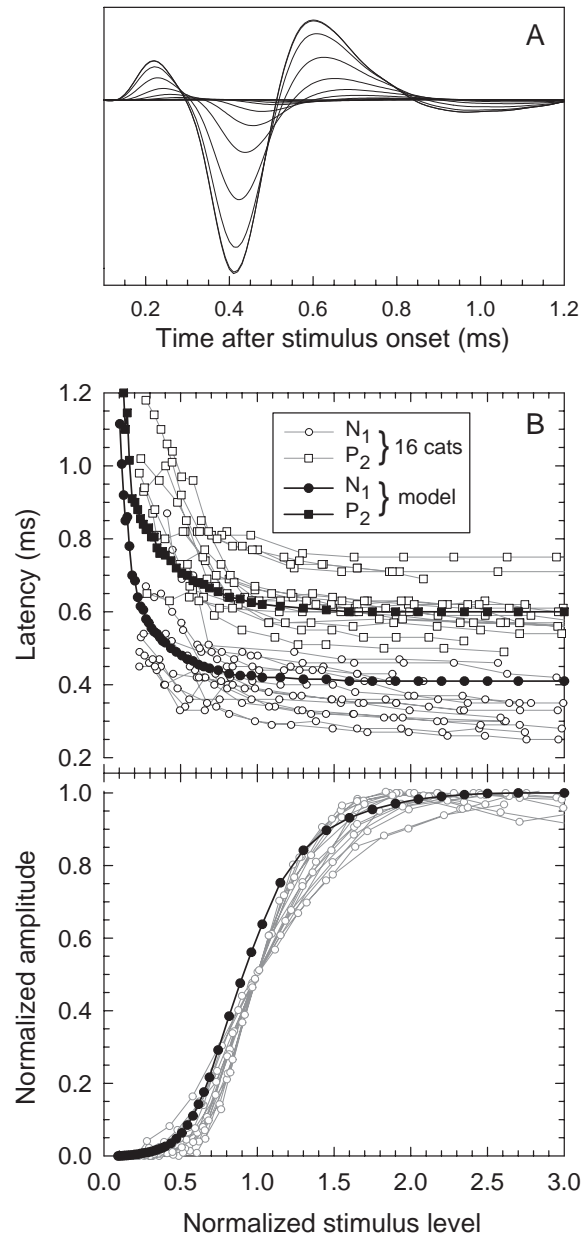


Figure 20: Derived EAP waveforms (upper graph) and input-output functions (lower graphs) produced by the phenomenological model. Representative EAP waveforms obtained at several stimulus levels are shown in upper panel. In lower panels, modeled latency-level and amplitude-level functions are plotted with filled symbols, while experimental data from 16 cats are plotted with open symbols. The N1 peak is defined as the most negative point of the waveform and the P2 peak as the subsequent maximum.

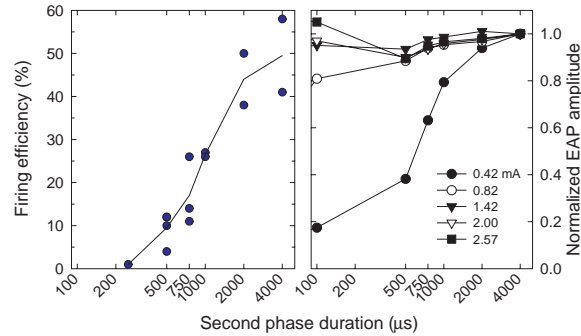


Figure 21: Comparison of EAP and single-fiber responses to pseudomonophasic pulses. On the right, EAP amplitude normalized to the monophasic pulse response amplitude is plotted as a function of second phase duration. Current level of the first pulse is the parameter. On the left, firing efficiency of a single fiber is plotted as a function of second phase duration. For both graphs, duration of the first pulse is always $40 \mu\text{s}$. In all cases, the level of the second phase was adjusted to maintain charge balance.

including jitter, RS, latency, and spike amplitude. Initial analyses suggest that refractory reductions in spike amplitude may be the most important of these factors. Data from the biophysical neuron model (discussed in Section 4.2) simulates a decreased spike amplitude as well as a slower recovery time for amplitude relative to spike rate, consistent with the EAP data in Figure 22.

4.2 Biophysical model of the auditory nerve: single units

The single-unit data described in section 3 has required us to modify our previous model parameters to maintain "physiologic" properties. The jitter and RS measures demonstrate that auditory neurons are "noisier" than our previous parameters would predict. It has been necessary to decrease the number of voltage-sensitive sodium channels at each node of Ranvier by a factor of ten to reproduce RS values of 4- 7%. While this seems like an extraordinary parameter change, the resulting channel density is still within reasonable bounds (Keynes, 1998) due to the requisite alteration of nodal axon diameter. These alterations preserve physiologic conduction velocity (see Section 2.7), spike shape, spike amplitude and threshold. They cannot however, explain the after-hyperpolarization seen in some of the better quality single-unit recordings. This finding is likely due to a delayed-rectifying

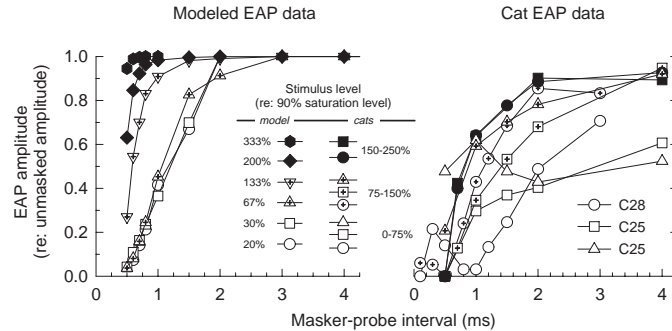


Figure 22: Comparison of EAP and modeled refractory recovery data. Both graphs plot EAP amplitude normalized to the unmasked amplitude as a function of interpulse interval. Cat EAP data, plotted on the right, display examples from three animals, each at three stimulus levels. Level is shown in the legend, indicated as the level relative to the level producing a response amplitude 90% of the saturation amplitude. Model data plotted on the left is plotted for six stimulus levels similarly indicated in the legend relative to the 90% saturation level. Details of the model are explained in the text as well as in Miller et al. (1999b).

potassium channel. We have incorporated such a channel into the model and representative spikes are shown in Figure 23. In other neurons, such delayed potassium currents serve to shorten the refractory period (Stutman, 1993); given that the model's absolute refractory period is still approximately 70% too long, it is reasonable to expect that more accurate refractory characteristics are produced by this modification.

4.3 Biophysical model of the auditory nerve: EAP

The biophysical model reproduces EAP activity that closely resembles the experimentally obtained measures. Figure 24 demonstrates model simulations of the EAP recorded from the cochlea and directly from the auditory nerve. The different response morphologies associated with recording at these two sites is apparent. Intracochlear recordings are uniformly biphasic, while direct-nerve recordings can be triphasic. Model simulations have also demonstrated effects of stimulus polarity, similar to those shown in Figure 1. Biphasic waveforms recorded with anodic stimuli are consistent with our model simulations, suggesting that biphasic EAPs occur when the excitation site is within four nodes of Ranvier of the recording site, a situation more likely with anodic stimulation. Such mechanistic insight into our ex-

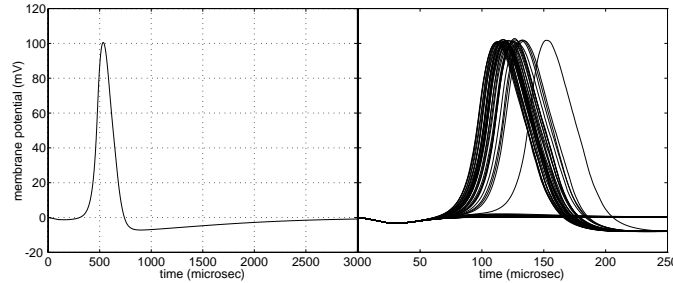


Figure 23: Representative single-fiber action potentials produced by the biophysical model with incorporation of delayed-rectifying potassium channels. After-hyperpolarization is seen in the single action potential on the left trace; the right graph provides an expanded time scale and multiple near threshold stimuli.

perimental results is an example of the utility of our modeling efforts.

4.4 Manipulation of membrane noise properties

Some of the more intriguing findings of these modeling efforts describe stimulus modifications that alter noise properties of the membrane. Figure 25 illustrates simulated input-output functions for the second pulse of a two-pulse stimulus. The first pulse is of an intensity sufficient to evoke a firing efficiency of 100%; the interpulse interval is the parameter. It is clear that the RS and dynamic range of the simulation are dependent on the IPI, demonstrating a ten-fold increase in the RS over a very short range of IPIs. EAP measures in cats are consistent with this finding (Rubinstein et al., 1997), but its potential importance for determining optimum stimulation rates warrants single-unit investigation.

Another way to manipulate membrane noise is demonstrated by the use of high-rate pulse train stimuli to generate spike activity similar to normal spontaneous activity (Rubinstein et al., 1998a,b). Figure 26 illustrates the interval histograms for a simulated fiber under the influence of a 5 kHz pulse train. The parameter is the stimulus amplitude. Such histograms closely resemble those produced by spontaneous activity in the normal cochlea; they reflect a Poisson process with dead time, or renewal process. Extensive statistical analysis (Rubinstein et al., 1999; Rubinstein et al., 1998a) shows that this activity is indistinguishable from true spontaneous activity and it has thus been termed “pseudospontaneous activity”. Measures of the EAP performed here (Matsuoka et al., 1998) and at Research Triangle

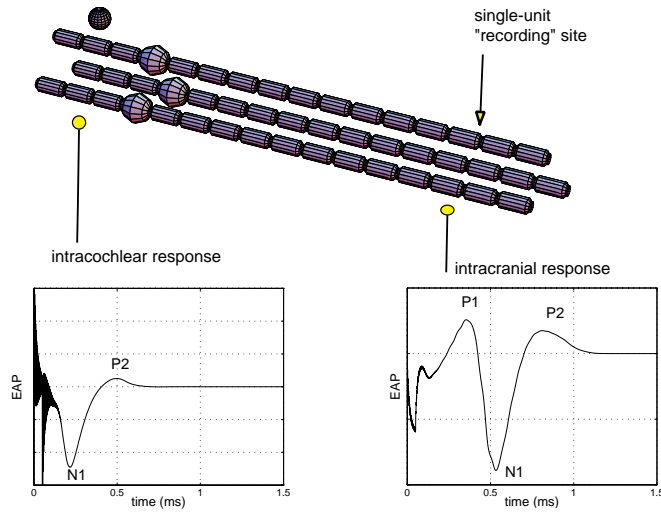


Figure 24: Modeled EAP responses obtained at two different recording sites relative to the modeled fibers. The “intracochlear” response was obtained with the recording site located near the peripheral processes, while the “intracranial” response was recorded near the central axonal processes.

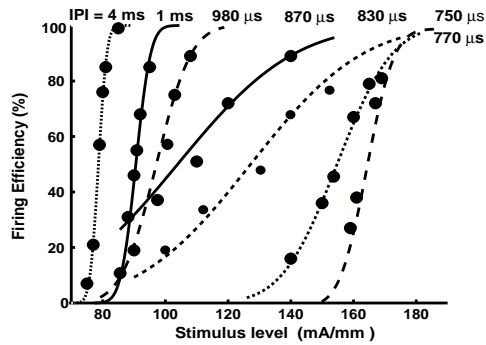


Figure 25: Input-output functions for a model node of Ranvier during the relative refractory period. Simulated on the Cray C90 at the San Diego Supercomputer Center.

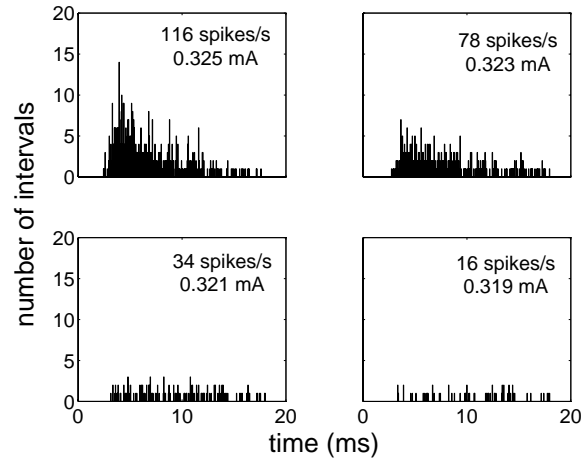


Figure 26: Interval histograms of a simulated fiber. The histograms were obtained under four different levels of a 5 kHz pulse train conditioner that acted to elicit “pseudospontaneous” activity.

Institute (Rubinstein et al., 1999) are consistent with this theory. The data suggest that a potentially important feature of normal auditory coding may be restored with appropriate speech processing algorithms. Such strategies would involve mixing “conditioning” pulse trains with a lower-rate speech stimulus.

When these “conditioning” pulse trains are combined with electrical sinusoids, two important features of acoustic stimulation are reproduced in the modeled fibers. First, the dynamic range for the sinusoid stimulus is increased from 1-2 dB to 20-25 dB, as illustrated in Figure 27. Second, the period histograms for the sinusoid closely resemble those seen with acoustic stimulation, as demonstrated in Figure 28. Electrophysiologic results using conditioning pulses in a human subject are described in the following section.

5 Human studies

Our work with human implant patients has primarily been performed as part of a larger program project (Iowa Cochlear Implant Project, Bruce Gantz, P.I.). Much of that work is focused on using the electrically evoked potentials to better understand the bases for differences in performance among individuals. We have also explored the relationship between residual hear-

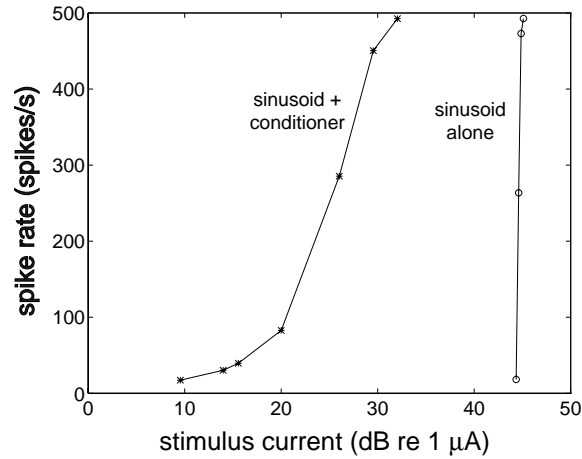


Figure 27: Model simulations of fiber rate-level functions obtained both with (left plot) and without (right plot) the presence of a 5 kHz pulse-train conditioning stimulus.

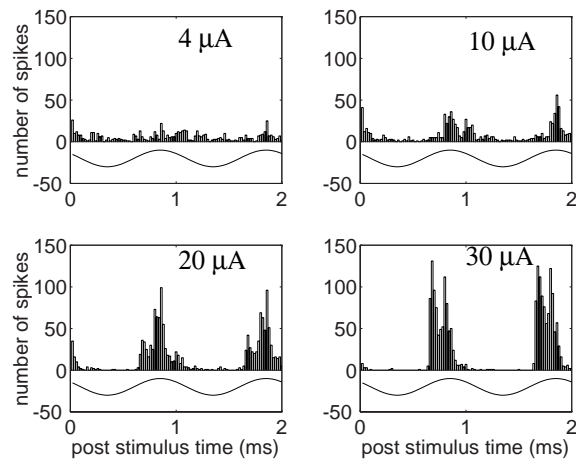


Figure 28: Model simulation of a period histogram in response to sinusoidal stimulation at the indicated current levels with simultaneous presentation of hi-rate conditioning pulses. The sinusoidal stimulus is shown at the bottom of each histogram.

ing, duration of deafness, and speech reception with an implant. Such information may then be used to adjust stimulation parameters to improve performance.

We have conducted several studies examining relationships between the EAP, EABR, and psychophysical measures (Abbas and Brown, 1991a,b; Brown et al., 1996, 1997). These and other measures of the EAP in human subjects (e.g., Finley et al., 1995; Wilson et al., 1997a,b) demonstrate the feasibility of obtaining such measures from implant users. The degree of correlation with psychophysical listening tasks suggests that these measures may be relevant to implant performance and clinical device-fitting strategies. Investigations using the EAP measures in the choice of electrode configuration or stimuli in an attempt to increase performance with the implant are ongoing in our laboratory. More recent measures of the EAP have used the Nucleus CI24M device which includes a telemetry system for measuring the intracochlear EAP (Brown et al., 1998; Abbas et al., 1999). The success with this new system and developments by other manufacturers (Karunasiri and McArthur, 1998), hold promise for the use of intracochlear recording techniques in a larger number of implant users than is presently possible.

During this contract, we have strengthened our collaboration with Research Triangle Institute and jointly developed the concept of conditioning stimuli to elicit pseudospontaneous activity. Figure 29 shows the effects of a high rate conditioning stimulus on the EAP representation of a vowel token in a human implant subject. The figure shows that stimulus pulse amplitude is distorted by refractory effects in the auditory nerve in the absence of conditioning. This effect is similar to what we have seen with sinusoidally amplitude modulated pulse trains at high modulation depth. When a conditioning stimulus is added, a more faithful representation of the vowel waveform is obtained. This result is precisely what was predicted a priori by our computational model. Preliminary speech testing with this approach has not yet documented statistically significant improvements in speech perception, but results are promising.

6 Summary

During the current contract period (i.e., 9/30/96 to the present), we have made significant progress in defining the single-unit and EAP responses to single-pulse electrical stimulation as well as the relationship between these two measures. We have defined differences between the EAP in cats and

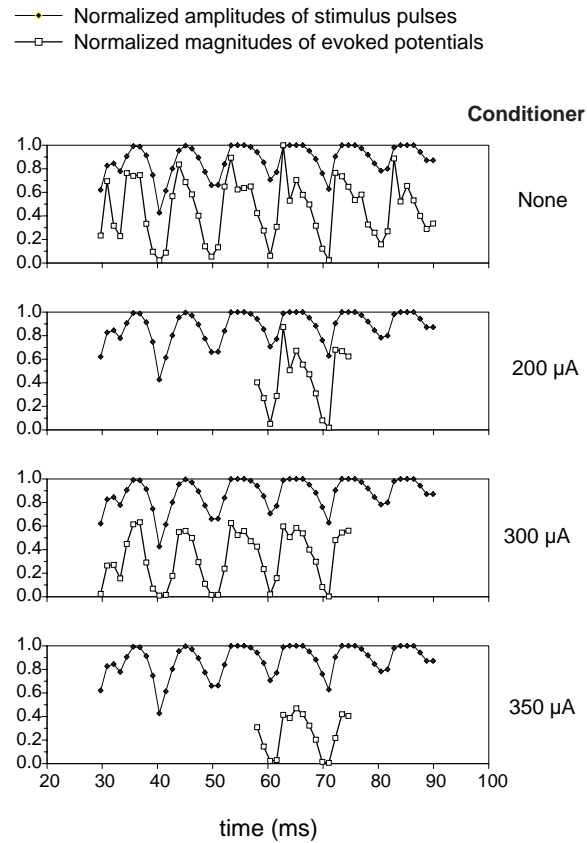


Figure 29: The effects of a high-rate conditioning stimulus on the EAP representation of a vowel token obtained from a human implant subject. Note that as the intensity of the conditioner increases, the neural response more faithfully represents the speech stimulus waveform. This figure is courtesy of Blake Wilson and Charles Finley and was obtained under their Neural Prosthesis Program contract.

guinea pigs. We have made preliminary measures of channel interactions with two multi-electrode arrays. We have examined the EAP response to modulated and unmodulated pulse trains in both species. Extensive analysis of our computational model has been performed in coordination with these experiments and has also directed us to potentially fruitful manipulations of speech processing strategies to improve neural representation of prosthetically delivered stimuli.

7 Publications and patents

During the past three years, eight manuscripts have been submitted to peer-reviewed journals from work funded partially by this contract. We have also applied for three patents. These efforts are listed below.

- Miller, C.A., Abbas, P.J., Rubinstein, J.T., Robinson, B.K., Matsuoka, A.J., & Woodworth, G. (1998). Electrically evoked compound action potentials of guinea pig and cat: responses to monopolar, monophasic stimulation. *Hear. Res.*, 119, 142-154.
- Rubinstein, J.T., Wilson, B.S., Finley, C.C. & Abbas, P.J. (1999). Pseudospontaneous activity: stochastic independence of auditory nerve fibers with electrical stimulation. *Hear. Res.*, 127,108-118.
- Miller, C.A., Abbas, P.J., Robinson, B.K., Matsuoka, A.J. & Rubinstein, J.T. (1999). Electrically evoked single-fiber action potentials from cat: responses to monopolar, monophasic stimulation. *Hear Res.*, 130, 197-218.
- Rubinstein, J.T. & Miller, C.M. (1999). How do cochlear prostheses work? *Current Opinion in Neurobiology*, 9, 399-404.
- Miller, C.A., Abbas, P.J. & Rubinstein, J.T. (1999). An empirically based model of the electrically evoked compound action potential. *Hear Res.*, 135, 1-18.
- Matsuoka, A.J., Abbas,P.J., Miller, C.A. & Rubinstein, J.T. (submitted). The neuronal response to electrical constant-amplitude pulse train stimulation: Additive Gaussian noise. *IEEE Transactions on Biomedical Engineering*

- Matsuoka, A.J., Rubinstein, J.T., Abbas,P.J. & Miller, C.A. (submitted). The effects of interpulse interval on stochastic properties of electrical stimulation: Models and Measurements. IEEE Transactions on Biomedical Engineering
- Matsuoka, A.J., Abbas,P.J., Rubinstein, J.T., & Miller, C.A. (submitted). The neuronal response to electrical constant-amplitude pulse train stimulation: Evoked compound action potential recordings. IEEE Transactions on Biomedical Engineering
- Rubinstein, J.T. Pseudospontaneous neural stimulation system and method. U.S. patent application No. 09/023278.
- Rubinstein, J.T. & Wilson BS. Speech processing system and method using pseudospontaneous stimulation. U.S. patent application No. 09/023279.
- Rubinstein JT, Brown CJ, Tyler RS, Abbas PJ. System and method for application of pseudospontaneous neural stimulation. U.S. patent application No. 09/373785

In addition to these publications and patents, we have published or submitted the following eighteen manuscripts during the contract period that were not funded by our contract. Studies that involve human subjects are relevant to questions we address and document our ability to transfer technologic developments to clinical applications.

- Rubinstein, JT, Parkinson, W.S., Lowder, M.W., Gantz, B.J., Nadol, J.B. Jr. & Tyler, R.S. (1998). Single- channel to multichannel conversions in adult cochlear implant patients. *Am. J. Otol.*, 19, 461–466.
- Rubinstein, J.T., Gantz, B.J. & Parkinson, W.S. Management of cochlear implant infections. *Am. J. Otol.* 20: 46–49, 1999.
- Rubinstein, J.T., Parkinson, W.S., Tyler, R.S. & Gantz, B.J. (1999). Residual speech recognition and cochlear implant performance: effects of implantation criteria. *Am. J. Otol.*, 20, 445–452.
- White JA, Rubinstein JT, Kay A. (in press) Intrinsic noise in neurons. *Trends in Neuroscience*, 1999.

- Gantz, B.J., Rubinstein, J., Tyler, R., Teagle, H., Cohen, N., Waltzman, S., Miyamoto, R. & Kirk, K. (in press). Long term results of cochlear implants in children with residual hearing. *Ann. Otol Rhinol. Laryngol.*
- Gantz, B.J., Perry, B. & Rubinstein, J.T. (in press). Cochlear Implants. *Clinical Otology.*
- Yoo S.K., Wang G., Rubinstein J.T., Skinner M.W., Vannier M.W. (in press) Three-dimensional modeling and visualization of the cochlea on the internet. *IEEE Trans. Info Tech. Biomed.*
- Yang S., Wang G., Skinner M.W., Rubinstein J.T., Vannier M.W. (in press) Localization of dense markers in radiographs. *Medical Physics.*
- Wang, G., Skinner, M.W., Rubinstein, J.T., Howard, M.A. & Vannier, M.W. (submitted). Digital X-ray stereophotogrammetry for cochlear implantation. *IEEE Trans. Biomed. Engin.*
- Brown, C.J., Abbas, P.J., Borland, J., & Bertschy, M.R. (1996). Electrically evoked whole nerve action potentials in Ineraid cochlear implant users: Responses to different stimulating electrode configurations and comparison to psychophysical responses. *J. Speech Hear. Res.*, 39. 453-467.
- Howard, M.A., Volkov, I., Abbas, P., Damasio, H., Ollendieck, M. & Granner, M. (1996). A chronic microelectrode investigation of the tonotopic organization of human auditory cortex. *Brain Res.*, 724, 260-264.
- Abbas, P.J. (1997). Adaptation in the auditory system. In M. Crocker (Ed.), *Encyclopedia of Acoustics.*
- Zhang, M. & Abbas, P.J. (1997). Effects of middle ear pressure on otoacoustic emission measures. *J. Acoust. Soc. Am.* , 102, 1032-1037.
- Abbas, P.J. & Miller, C.A. (1998). Physiology of the auditory system. In Cummings, Fredrickson, Harker, Krause, & Schuller (Eds.), *Otolaryngology - Head and Neck Surgery (3rd Ed.)*. St. Louis, MO: CV Mosby Co.
- Abbas, P.J. & Brown, C.J. (in press). Electrophysiology and device telemetry. Cochlear Implants S. Waltzman and N. Cohen (eds.).

- Brown, C.J., Hughes, M.L., Lopez, S.M. & Abbas, P.J. (1999). The relationship between EABR thresholds and levels used to program the Clarion speech processor. *Ann. Otol. Rhinol. Laryngol.*
- Brown, C.J., Abbas, P.J. & Gantz, B.J. (1998). Auditory nerve potentials recorded using the neural response telemetry system of the Nucleus CI24M cochlear implant. *Am. J. of Otol.* 19, 320-327.
- Abbas, P.J., Brown, C.J., Shallop, J.K., Firszt, J.B., Hughes, M.L., Hong, S.H. & Staller, S.J. (1999). Summary of results using the Nucleus CI24M implant to record the electrically evoked compound action potential. *Ear and Hearing.*, 20, 45-59.

References

- [1] Abbas P.J., & Brown C.J. (1991a). Electrically evoked auditory brainstem response: Growth of response with current level. *Hear. Res.*, 51, 123-137.
- [2] Abbas P.J., & Brown C.J. (1991b). Electrically evoked auditory brainstem response: Refractory properties and strength-duration functions. *Hear. Res.*, 51, 139- 147.
- [3] Abbas P.J., Miller C.A., Matsuoka A.J., & Rubinstein J.T. (1997b). The neurophysiological effects of simulated auditory prosthesis stimulation. Fourth Quarterly Progress Report N01-DC-6-2111.
- [4] Abbas P.J., Brown C.J., Shallop J.K., Firszt J.B., Hughes M.L., Hong S.H., & Staller S.J. (1999). Summary of results using the Nucleus Ci24M implant to record the electrically evoked compound action potential. *Ear & Hearing.*
- [5] Arnesen A.R., & Osen K.K. (1978). The cochlear nerve in the cat: Topography, cochleotopy, and fiber spectrum. *J. Comp. Neurol.*, 178, 661-678.
- [6] Bostock H. (1983). The strength-duration relationship for excitation of myelinated nerve: Computed dependency on membrane parameters. *J. Physiol.*, 341, 59-74.
- [7] Brismar T. (1980). Potential clamp analysis of membrane currents in rat myelinated nerve fibers. *J. Physiol.*, 298, 171-184.

- [8] Brown C.J., Abbas P.J., Borland J., & Bertschy M.R. (1996). Electrically evoked whole nerve action potentials in Ineraid cochlear implant users: Responses to different stimulating electrode configurations and comparison to psychophysical responses. *J. Speech Hear. Res.*, 39, 453-467.
- [9] Brown C.J., Abbas P.J., & Gantz B.J. (1998). Auditory nerve potentials recorded using the neural response telemetry system of the Nucleus CI24M cochlear implant. *Am. J. Oto.*, 19, 320-327.
- [10] Burgess P.R., & Perl E.R. (1973). Cutaneous mechanoreceptors and nociceptors. In A. Iggo (Ed.), *Handbook of sensory physiology, the somatosensory system*. New York: Springer-Verlag.
- [11] Finley, C.C., Wilson, B.S., van den Honert, C., and Lawson, D.T. (1997). Sixth Quarterly Progress Report, Speech Processors for Auditory Prostheses, NIH Contract N01- DC-5-2103.
- [12] Goldstein M.H., & Kiang N.Y.-S. (1958). Synchrony of neural activity in electric response evoked by transient acoustic stimuli. *J. Acoust. Soc. Am.*, 30, 107-114.
- [13] Hartmann R., & Klinke R. (1990). Response characteristics of nerve fibers to patterned electrical stimulation. In J.M. Miller & F.A. Spelman (Eds.), *Cochlear implants: Models of the electrically stimulated ear* (pp. 135-160). New York: Springer-Verlag.
- [14] Hall R.D. (1990). Estimation of surviving spiral ganglion cells in the deaf rat using the electrically evoked auditory brainstem response. *Hear. Res.*, 45, 123-136.
- [15] Hill A.V. (1936). Excitation and accommodation in nerve. *Proceed. Royal Society of London. Series B: Biological Sciences.*, 119, 305-355.
- [16] Hong, S.H., Brown, C.J., Hughes, M.L., and Abbas. P.J. (1998). Electrically evoked compound action potentials using neural response telemetry in CI24M: Refractory recovery function of the auditory nerve. Abstracts ARO 1998 Midwinter Meeting, St Petersburg Beach, FL
- [17] Hursh J.B. (1939). Conduction velocity and diameter of nerve fibers. *Am. J. Physiol.* 127, 131-139.

- [18] Javel E. (1990). Acoustic and electrical encoding of temporal information. In J.M. Miller & F.A. Spelman (Eds.), *Models of the electrically stimulated cochlea*. New York: Springer-Verlag.
- [19] Javel E., Tong Y.C., Shepherd R.K., & Clark G.M. (1987). Responses of cat auditory nerve fibers to biphasic electrical current pulses. *Ann. Otol. Rhinol. Laryngol.*, 96 (Suppl. 128), 26-30.
- [20] Karunasiri T., & McArthur, P. (1998). Custom IC designs for neural response measurements. Abstracts from First International Symposium and Workshop on Objective Measures in Cochlear Implantation, Nottingham, UK.
- [21] Keynes R.D. (1998). The design of peripheral nerve fibers. In: *Principle of animal design*, Eds. E.R. Weibel, C.R. Taylor and L. Bolis, Cambridge University Press: Cambridge.
- [22] Kiang N.Y.S., Moxon, E.C. and Kahn A.R. (1976). The relationship of gross potentials recorded from the cochlea to single-unit activity in the auditory nerve. In R.J. Rubin, C. Elberling and G. Salomon (eds) *Electrocochleography* Baltimore, University Park.
- [23] Liberman C., & Oliver M.E. (1984). Morphometry of intracellularly labeled neurons of the auditory nerve: Correlations with functional properties. *J. Comp. Neurol.*, 223, 163-176.
- [24] Matsuoka A.J., Abbas P.J., Rubinstein J.T., & Miller C.A. (1998). The neurophysiological effects of simulated auditory prosthesis stimulation. Seventh Quarterly Progress Report N01-DC-6-2111.
- [25] Miller C.A., Abbas P.J., & Robinson, B.K. (1994). The use of long-duration current pulses to assess nerve survival. *Hear. Res.*, 78, 11-26.
- [26] Miller C.A., Abbas P.J., & Rubinstein J.T. (1999b). An empirically based model of the electrically evoked compound action potential. *Hear. Res.*, 135, 1-18.
- [27] Miller C.A., Abbas P.J., Rubinstein J.T., Robinson B.K., & Matsuoka A.J. (1999a) Electrically evoked single-fiber action potentials from cat: responses to monopolar, monophasic stimulation. *Hear. Res.*, 130, 197-218.

- [28] Miller C.A., Abbas P.J., Rubinstein J.T., Robinson B.K., Matsuoka A.J., & Woodworth G. (1998b) Electrically evoked compound action potentials of guinea pig and cat: response to monopolar, monophasic stimulation. *Hear. Res.*, 119, 142-154.
- [29] Rattay F. (1989). Analysis of models for extracellular fiber stimulation. *IEEE Trans. Biomed Engin.* 36, 676-682.
- [30] Rubinstein J.T. (1993). Axon termination conditions for electrical stimulation. *IEEE Transactions on Biomed. Eng.*, 40(7), 654-663.
- [31] Rubinstein J.T. (1995). Threshold fluctuations in an N Sodium Channel Model of the Node of Ranvier. *Biophysical J.*, 68, 779-785.
- [32] Rubinstein J.T., Matsuoka A.J., Abbas P.J., & Miller C.A. (1997). The neurophysiological effects of simulated auditory prosthesis stimulation. Second Quarterly Progress Report N01-DC-6-2111.
- [33] Rubinstein J.T., Parkinson W.S., Lowder M.W., Gantz B.J., Nadol J.B. Jr. and Tyler R.S. (1998a). Single-channel to multichannel conversions in adult cochlear implant subjects. *Am. J. Otol.* 19, 461-466.
- [34] Rubinstein J.T., Abbas P.J., Miller C.A., & Matsuoka A.J. (1998b). The neurophysiological effects of simulated auditory prosthesis stimulation. Eighth Quarterly Progress Report N01-DC-6-2111.
- [35] Rubinstein J.T., Wilson B.S., Finley C., & Abbas P.J. (1999a). Pseudospontaneous activity: stochastic independence of auditory nerve fibers with electrical stimulation. *Hear. Res.* 127, 108-118.
- [36] Smith, D.W., Finley, C.C., van den Honert, C., Olszyk, V.B., Konrad, K.E.M., Behavioral and electrophysiological responses to electrical stimulation in the cat I. Absolute thresholds, *Hear. Res.* 81, 1-10.
- [37] Stutman E.R. (1993). A model for temporal sensitivity of neurons in the auditory brainstem. Masters thesis. Department of Biomedical Engineering, Boston University.
- [38] van den Honert C., & Stypulkowski P.H. (1987). Temporal response patterns of single auditory nerve fibers elicited by periodic electrical stimuli. *Hear. Res.*, 29, 207-222.

- [39] Verveen A.A. (1961). Fluctuation in Excitability, Drukkerij Holland N.V., Amsterdam. Wang B. (1979). The relation between the compound action potential and unit discharges of the auditory nerve. Ph.D. Thesis, MIT, Cambridge MA.
- [40] Wang B., & Kiang N.Y.S. (1978). Synthesized compound action potentials (CAPs) of the auditory nerve. *J. Acoust. Soc. Am.*, 63(Suppl.), S77.
- [41] Weibel E.R. (1979). *Stereological methods: Vol. 1 - Practical methods for biological morphometry*. New York: Academic Press.
- [42] Weibel, C.R. Taylor and L. Bolis. Cambridge University Press: Cambridge, 271-277.
- [43] Wilson B.S., Finley C.C., Zerbi M., & Lawson, D. (1995). Eleventh Quarterly Progress Report, Speech Processors for Auditory Prosthesis, NIH Contract N01-2-2401, Center for Auditory Prosthesis Research.
- [44] Wilson B.S. (1997). The future of cochlear implants. *British Journal of Audiology*, 31, 205-225.
- [45] Wilson B.S., Finley C.C., Lawson D.T. & Zerbi M. (1997a). Temporal representations with cochlear implants. *Am. J. Otol.*, 18, S30-34.
- [46] Wilson B.S., Zerbi M., Finley C.C., Lawson D.T. & van den Honert, C. (1997b). Speech processors for auditory prostheses. Seventh Quarterly Progress Report, NIH Contract N01-DC-5-2103.